

Resistance and Heat Transfer Laws for Stable and Neutral Planetary Boundary Layers: Old Theory Advanced and Re-evaluated

Sergej S. Zilitinkevich^{1,2,3} and Igor N. Esau²

¹ Division of Atmospheric Sciences, Department of Physical Sciences, University of Helsinki, Finland (postal address: FMI, Vuorikatu 15 A, P.O. Box 503, 00101 Helsinki, Finland; Tel. +358-9-1929-4678; E-mail Sergej.Zilitinkevich@fmi.fi)

² Nansen Environmental and Remote Sensing Centre / Bjerknes Centre for Climate Research, Bergen, Norway

³ Air-Water Science Programme, Department of Earth Sciences, Uppsala University, Sweden

Submitted to

***Quarterly Journal of the Royal
Meteorological Society***

Final version, 14 February 2005

Resistance and Heat Transfer Laws for Stable and Neutral Planetary Boundary Layers: Old Theory Advanced and Re-evaluated

Sergej S. Zilitinkevich^{1,2,3} and Igor N. Esau²

¹ Division of Atmospheric Sciences, Department of Physical Sciences, University of Helsinki, Finland (postal address: FMI, Vuorikatu 15 A, P.O. Box 503, 00101 Helsinki, Finland; Tel. +358-9-1929-4678; E-mail Sergej.Zilitinkevich@fmi.fi)

² Nansen Environmental and Remote Sensing Centre / Bjerknes Centre for Climate Research, Bergen, Norway

³ Air-Water Science Programme, Department of Earth Sciences, Uppsala University, Sweden

Abstract

The planetary boundary layer (PBL) resistance and heat-transfer laws express the surface fluxes of momentum and heat through the PBL governing parameters. Since the late sixties, the dimensionless coefficients (A , B and C) in these laws were considered as single-valued functions of internal stability parameters: $\mu = u_* / |f| L_s$ in the steady state PBLs, or h/L_s in the evolving PBLs (u_* is the friction velocity, f is the Coriolis parameter, L_s is the Monin-Obukhov length, and h is the PBL depth). Numerous studies revealed very wide spread of data in empirical plots of A , B and C versus μ or h/L_s . It is not surprising that the above laws, although included in all modern textbooks on boundary-layer meteorology, are not practically used. In the present paper the resistance and heat-transfer laws are revised accounting for the free-flow stability, baroclinicity and the rise of capping inversion. The coefficients A , B and C become functions not only of μ or h/L_s , but also of the external stability parameter $\mu_N = N / |f|$ (where N is the Brunt Väisälä frequency in the free atmosphere above the PBL), the parameter of baroclinicity $\mu_\Gamma = \Gamma / N$ (or the free-flow Richardson number $Ri = (N/\Gamma)^2 = \mu_\Gamma^{-2}$, where Γ is the geostrophic wind shear), and the ratio h/h_E of the actual h and the equilibrium h_E PBL depths. Moreover the coefficient C is redefined to account for the effect of capping inversion. It follows that A , B and C can be considered as single-valued functions of μ only in the steady-state, barotropic, nocturnal (that is short-lived) PBL. On the contrary, the advanced laws cover a wide range of the PBL regimes. They are validated through large-eddy simulation (LES) of different types of PBLs: truly neutral, conventionally neutral, nocturnal and long-lived. This new development explains why prior formulations performed so poor and promotes advanced resistance and heat transfer laws as a practical tool for use in environmental modelling applications.

1. Introduction

The resistance laws for the barotropic planetary boundary layer (PBL) are presented in modern textbooks on boundary-layer meteorology (e.g., Garratt, 1992) and comprehensively discussed in recent papers of Hess and Garratt (2002a,b) and Zilitinkevich and Esau (2002); so they do not require detailed introductory explanations. These laws express the absolute value of the surface stress $|\bar{\tau}|_{z=0} = u_*^2$ (u_* is the friction velocity, and z is the height) and the cross-isobaric angle α (the angle between that surface stress and the geostrophic wind) through the PBL governing parameters:

$$\frac{k}{C_g} \cos \alpha = \ln(C_g \text{Ro}) - \tilde{A}, \quad \frac{k}{C_g} \sin \alpha = \mp \tilde{B}, \quad (1)$$

where C_g and Ro are the geostrophic drag coefficient and the surface Rossby number:

$$C_g = \frac{u_*}{G}, \quad \text{Ro} = \frac{G}{|f| z_{0u}}. \quad (2)$$

Here, k is the von Karman constant (conventional value: $k=0.4$), \tilde{A} and \tilde{B} are dimensionless coefficients, f is the Coriolis parameter, z_{0u} is the surface roughness length for momentum, G is the geostrophic wind speed: $G^2 = u_g^2 + v_g^2$, $u_g \equiv -(\rho f)^{-1} \partial p / \partial y = G \cos \alpha$ and $v_g \equiv (\rho f)^{-1} \partial p / \partial x = G \sin \alpha$ are the geostrophic wind components (depth-constant in the barotropic PBL), ρ is the air density, and p is the atmospheric pressure. On the right hand side (r.h.s.) of Eq. (1b), minus is applied to the Northern Hemisphere and plus to the Southern Hemisphere. Equations (1) correspond

The potential-temperature resistance law analogous to Eq. (1) reads

$$\frac{k_T}{C_{TR}} = \ln(C_g \text{Ro}) - \tilde{C}, \quad C_{TR} = \frac{\theta_*}{\Delta \theta_{PBL}}, \quad (3)$$

where k_T is the von Karman constant for the temperature (conventional value: $k_T=0.4$), \tilde{C} is the same type of dimensionless coefficient as \tilde{A} and \tilde{B} , C_{TR} is the thermal resistance coefficient, $\theta_* = -F_{\theta} u_*^{-1}$ is the temperature scale based on the near-surface turbulent flux of potential temperature $F_{\theta}|_{z=0} = F_{\theta s}$, $\Delta \theta_{PBL} = \theta_h - \theta_0$ is the bulk increment in potential temperature across the boundary layer, $\theta_h = \theta|_{z=h}$ is the potential temperature at the PBL upper boundary (considered as given parameter), and θ_0 is the aerodynamic potential surface temperature.

The latter is defined through the logarithmic extrapolation of $\theta(z)$ down to the level $z = z_{0u}$. Needless to say, θ_0 differs from the actual surface temperature θ_s (often

referred to as the radiometric temperature). The difference $\theta_0 - \theta_s$ ranges up to several Kelvins over rough surfaces. Traditionally, it is expressed as

$$\frac{\theta_0 - \theta_s}{\theta_*} = \frac{1}{k_T} \ln \frac{z_{0u}}{z_{0T}}, \quad (4)$$

where z_{0T} is the roughness length for temperature (e.g., Zilitinkevich *et al.*, 2001). When z_{0T} becomes very uncertain (over partially vegetated land and some other very complex land surfaces) alternative approaches should be applied (see Mahrt and Vickers, 2002). In any case, introducing the aerodynamic surface temperature allows separate consideration of the thermal resistances of the two layers of essentially different nature:

- the PBL – in terms of $\Delta\theta_{PBL} = \theta_h - \theta_0$, Eq. (3),
- the roughness layer – in terms of $\theta_0 - \theta_s$, Eq. (4), or using other schemes.

The present paper focuses on the PBL resistance laws.

Equation (3) in combination with Eq. (1) provides the PBL heat transfer law:

$$F_{\theta_s} = -u_* \theta_* = -C_g C_{TR} G \Delta\theta_{PBL}. \quad (5)$$

Equations (1) for the neutral PBL (with \tilde{A} and \tilde{B} treated as universal constants: $\tilde{A} = \tilde{A}_0$ and $\tilde{B} = \tilde{B}_0$) were derived by Rossby and Montgomery (1935) from a turbulence closure model and later by Kazanski and Monin (1961) from more general similarity-theory reasoning. An overview of further studies of the resistance law for the atmospheric neutral PBL is given by Hess and Garratt (2002a,b) and Hess (2004).

Zilitinkevich *et al.* (1967) and Zilitinkevich and Chalikov (1968) extended Eq. (1) to the stratified PBLs affected by the non-zero buoyancy fluxes at the surface. They showed that \tilde{A} and \tilde{B} depend on the internal stability parameter μ based on the Monin-Obukhov length scale L_s :

$$\mu = \frac{u_*}{|f| L_s}, \quad L_s = \frac{-u_*^3}{\beta F_{\theta_s}}, \quad (6)$$

where $\beta = g/T$ is the buoyancy parameter, g is the acceleration due to gravity, and T is the absolute temperature. They also derived the temperature resistance law, Eq. (3), with \tilde{C} dependent on μ , and made the first attempt to empirically determine the resistance-law coefficients \tilde{A} , \tilde{B} , \tilde{C} and the similar type of coefficient \tilde{D} in the resistance law for humidity. In this context, the neutral stratification was defined as the regime in which μ is sufficiently small ($\mu < 10$). According to this point of view, the temperature flux F_{θ_s} could be non-zero (and the heat transfer law keeps it sense) when the stratification is practically neutral.

Zilitinkevich and Deardorff (1974) reformulated the resistance laws employing the actual boundary-layer depth h instead of the equilibrium PBL depth h_E [or its basic scale $u_* / |f|$] employed in Eqs. (1)-(3)]. The generalised laws read

$$\frac{k}{C_g} \cos \alpha = \ln \frac{h}{z_{0u}} - A, \quad \frac{k}{C_g} \sin \alpha = -\frac{fh}{u_*} B. \quad (7)$$

$$\frac{k_T}{C_{TR}} = \ln \frac{h}{z_{0u}} - C. \quad (8)$$

Here, the resistance-law coefficients A , B and C are considered as functions of h/L_s , rather than μ , which allows extending the theory to non-steady boundary layers with time/space-dependent depths¹. Equation (7b) is derived below in Section 2. In contrast to the prior formulation, $kC_g^{-1} \sin \alpha = \mp \tilde{B}$, it explicitly shows that the cross isobaric angle α is controlled by the Coriolis parameter f .

As for the stable stratification, all the above analyses were limited to the nocturnal PBLs, namely, the stable PBLs developed after the sun set on the background of much deeper residual layers, neutrally stratified due to intensive mixing during the day-time. In the steady-state, nocturnal PBL [when the PBL depth h is fully determined by u_* , f and L_s : $h = h_E = (u_* / |f|) f_h(\mu)$] Eqs. (7)-(8) reduce to Eqs. (1)-(3), wherein the coefficients A , B and C are expressed through \tilde{A} , \tilde{B} and \tilde{C} :

$$A = \tilde{A} + \ln \frac{|f| h_E}{u_*}, \quad B = \pm \frac{u_*}{f h_E} \tilde{B}, \quad C = \tilde{C} + \ln \frac{|f| h_E}{u_*}. \quad (9)$$

Zilitinkevich (1975) determined asymptotic behaviours of the resistance-law coefficients in Eqs. (1)-(3) and (7)-(8) at large values of μ and h/L_s , respectively.

In the truly neutral boundary layer, when the Monin-Obukhov length is large: $L_s \rightarrow \infty$ (so that $\mu, h/L_s \rightarrow 0$) and the static stability in the air flow above the PBL is neutral, the equilibrium boundary layer depth is expressed by the classical Rossby and Montgomery (1935) formula: $h_E = C_R u_* / |f|$, where C_R is a dimensionless constant ($C_R = 0.7$, after laboratory experiments and LES²). Then the resistance law coefficients

¹ Recall that convective PBLs never approach the steady state: they go on growing until the positive buoyancy flux is maintained. Contrastingly, stable PBLs tend to develop towards the steady state. The ratio h/h_E of the actual PBL depth, h , to the equilibrium stable PBL depth, h_E , is an important governing parameter for this type of turbulent boundary layers. Alternatively the deviation of the PBL from the steady state could be characterised by the dimensionless parameter $|f| h / u_*$ (Arya, 1975).

² Atmospheric data give much lower and very uncertain estimates of C_R (e.g. Tjernstrom and Smedman, 1993). This is due to the fact that the atmospheric boundary layers usually considered as neutral (according to the criteria $L_s \rightarrow \infty$ or $\mu \rightarrow 0$) are in fact only conventionally neutral. Zilitinkevich and Esau (2002) and Hess (2004) have demonstrated that their depths are strongly affected by the static stability in the free atmosphere.

$\tilde{A}_0, \tilde{B}_0, \tilde{C}_0$, $A_0 = \tilde{A}_0 + \ln C_R$, $B_0 = C_R^{-1} \tilde{B}_0$ and $C_0 = \tilde{C}_0 + \ln C_R$ become constants (the subscript “0” stands for the truly neutral stratification).

Since the late sixties, particular cases of the above laws were independently derived (e.g., by Gill, 1968), discussed and compared with experimental data in a large number of papers (see overviews in Byun, 1991; Zilitinkevich, 1989; Hess and Garratt, 2002a,b; Hess, 2004). In the majority of these works, the PBL is considered as neutral when μ or h/L_s is zero or sufficiently small. In the seventies and early eighties, much work focused on experimental determination of the resistance-law coefficients $\tilde{A}, \tilde{B}, \tilde{C}$ and \tilde{D} supposed to be single-valued functions of μ . However, empirical relationships of this type showed so wide spread of data that any interest in practical application of the resistance laws gradually decayed.

To some extent, large spread of data on empirical plots of the coefficients \tilde{A} and \tilde{B} was explained at the expense of baroclinicity (e.g., Arya and Wynggard, 1975; Joffre, 1982, 1984). The baroclinic correction to the resistance law was formulated in a linear approximation, neglecting the effect of baroclinic shear on turbulent mixing. It included the following two steps. First, employing the surface values of the geostrophic wind components ($u_{g0} = u_g|_{z=0}, v_{g0} = v_g|_{z=0}$), the barotropic resistance law (with \tilde{A} and \tilde{B} dependent on μ) was applied to determine u_* and the “barotropic part”, α , of the full wind-turn angle, $\alpha + \alpha_1$. Second, the “baroclinic part” of this angle, α_1 , was determined as the full turn of the geostrophic wind across the PBL. Recent version of this model and an overview of prior works are given by Djolov et al. (2004).

It was recognised long ago that not only baroclinicity, but the depth and the strength of the capping inversions and the static stability in the free atmosphere affect bulk features of stable PBLs (e.g., Csanady, 1973; Byun, 1991; Overland and Davidson, 1992; King and Turner, 1997). But the first attempts to quantify these effects were made only recently (Zilitinkevich *et al.*, 1998b; Zilitinkevich and Esau, 2002, 2003).

A new theoretical model presented in this paper goes further and extends the resistance and heat transfer laws to long-lived, stable PBLs accounting for the following mechanisms:

- damping effect of the static stability in the free atmosphere on the PBL turbulent length scale,
- development of capping inversions at the PBL upper boundary,
- enhancing effect of the baroclinic shear on the PBL turbulent velocity scale.

Prior models overlooked these mechanisms and therefore were applicable only to the nocturnal PBLs. This explains enormous spread of data points in old empirical plots of $\tilde{A}, \tilde{B}, \tilde{C}$ and \tilde{D} versus μ .

In this paper, the free atmosphere is characterised by the Brunt-Väisälä frequency, N , and the baroclinic shears, $\Gamma_u = \partial u_g / \partial z$ and $\Gamma_v = \partial v_g / \partial z$, which involve the dimensionless parameters of the external stability μ_N and baroclinicity μ_Γ :

$$\mu_N = \frac{N}{|f|}, \text{ where } N = \left(\beta \frac{\partial \theta}{\partial z} \right)^{1/2} \text{ at } z > h,$$

$$\mu_\Gamma = \frac{\Gamma}{N}, \text{ where } \Gamma = (\Gamma_u^2 + \Gamma_v^2)^{1/2} = \frac{g}{|f|T} \left[\left(\frac{\partial T}{\partial y} \right)^2 + \left(\frac{\partial T}{\partial x} \right)^2 \right]^{1/2}. \quad (10)$$

Alternatively, the role of baroclinicity can be characterised by the free-flow Richardson number $\text{Ri} = \mu_\Gamma^{-2}$. On the r.h.s. of Eq. (10) for Γ , the geostrophic shear is expressed through the large-scale horizontal temperature gradient using the thermal wind equation. N and Γ are taken depth-constant in a reasonable correspondence with real properties observations of the Earth's atmosphere: $N = 10^{-2} \text{ s}^{-1}$ and $\Gamma \sim (3-6) \cdot 10^{-3} \text{ s}^{-1}$ that correspond to $\mu_N \sim 10^2$ and $\mu_\Gamma \sim (3-6) \cdot 10^{-1}$.

Following Zilitinkevich and Esau (2003), the PBL baroclinic turbulent velocity scale u_T is defined as

$$u_T^2 = \frac{u_*^2}{1 - C_0 \text{Ri}^{-1/2}} \approx u_*^2 (1 + C_0 \text{Ri}^{-1/2}) = u_*^2 (1 + C_0 \mu_\Gamma), \quad (11)$$

where $C_0 = 0.67$ is a dimensionless constant determined through LES validation of the baroclinic PBL depth formulation³. In the barotropic PBLs, u_T reduces to the universally accepted scale u_* .

Accounting for the μ_N -dependence, Zilitinkevich and Esau (2002) have explained wide spread of empirical data on \tilde{A} and \tilde{B} , as well as a seemingly paradoxical disagreement between the atmospheric estimates and the LES, DNS or lab-experiment estimates of \tilde{A} and \tilde{B} in the boundary layers traditionally considered as neutral. The key point is that numerical or lab models deal with the truly neutral PBLs ($\mu = 0$ and $\mu_N = 0$), whereas atmospheric PBLs treated as neutral ($|\mu| \ll 10$) are nearly always strongly affected by the free-flow stability ($\mu_N \sim 10^2$). These two types of the PBL are essentially different in nature. To distinguish between them, Zilitinkevich and Calanca (2000) have proposed the following definitions: The PBL is called ‘‘conventionally neutral’’ when the buoyancy flux βF_θ approaches zero at the surface but the free flow above the PBL is stably stratified. When both the surface buoyancy flux βF_θ and the free flow Brunt Väisälä frequency N are zero, the PBL is called ‘‘truly neutral’’.

In the present paper the theory is further advanced and validated against new LES.

³ In the imaginary case that the free atmosphere is neutrally stratified ($N = 0$) but baroclinic ($\Gamma > 0$), the baroclinic shear causes the overall turbulisation, so that the very concepts of the turbulent boundary layer and the PBL turbulent velocity scale become inapplicable.

2. Theoretical model

2.1. TURBULENT LENGTH SCALES

Earlier versions of the resistance and heat transfer laws were derived through asymptotic matching of the near-surface profiles of the wind velocity components $u(z)$, $v(z)$ and the potential temperature $\theta(z)$ with the defect-functions $u(z) - u(h)$, $v(z) - v(h)$ and $\theta(z) - \theta(h)$ in the overlapping height interval $z_{0u} \ll z \ll h$. Thus the surface layer model represented an essential starting point of the theory.

Prior derivations employed the Monin-Obukhov (1954) similarity theory for the surface-layer profiles and the defect-functions based on the PBL-depth formulations of Rossby and Montgomery (1935) and Zilitinkevich (1972) – for the neutral and stable boundary layers, respectively.

This approach is justified when applied to nocturnal stable PBLs, namely, to the comparatively short-lived PBLs separated from the free flow by a neutrally stratified residual layer, which keeps memory of the day-time mixing. In such PBLs, except for the thin log-boundary layer close to the surface, the turbulent length scale is limited to the “local Monin-Obukhov length” L defined similarly to Eq. (6b) but employing local (z -dependent) values of the turbulent fluxes of momentum $\tau(z)$ and potential temperature $F_\theta(z)$ (Nieuwstadt, 1984).

More generally, including the truly neutral PBLs (in which $L^{-1} = 0$) and the long-lived stable PBLs (that is the PBLs bordering upon the stably stratified free atmosphere, without any intermediate residual layer), the turbulent length scales are restricted by the following alternative limits: local (z -dependent) static stability scale L , non-local external static stability scale L_N , and the rotational scale L_f , namely,

$$L = \frac{\tau^{3/2}}{-\beta F_\theta}, \quad L_N = \frac{u_*}{N}, \quad L_f = \frac{u_*}{|f|}. \quad (12)$$

In baroclinic PBLs, the baroclinic turbulent velocity scale u_T , Eq. (11), should be substituted for u_* in the above expression for L_N .

The scales L and L_N are inherent to the nocturnal and to the conventionally neutral PBLs and reflect the damping effect on turbulence of the turbulent buoyancy flux within the PBL and the static stability in the free flow, respectively. Clearly, in each concrete case the basic role is played by the stronger effect, that is by the smaller scale: L , L_N or L_f . Moreover, their relative importance is different at different heights because L depends on z through the dependences $\tau(z)$ and $F_\theta(z)$.

In further analysis, we employ a recently created LES data base representing three different types of the stable PBL: nocturnal, long-lived and conventionally neutral, and the truly neutral PBL (see Section 3). LES data shown in Figure 1 demonstrates

that the normalised fluxes of momentum and potential temperature can to a reasonable accuracy be considered as self-similar functions of the dimensionless height $\zeta = z/h$:

$$\frac{\tau}{u_*^2} = f_\tau(\zeta), \quad \frac{F_\theta}{F_{\theta_s}} = f_{F_\theta}(\zeta). \quad (13)$$

As shown in Appendix, such a self-similarity is consistent with scaling analysis of the Ekman equations. It has been disclosed in prior analyses of field data (e.g., Sorbjan, 1988; Lenshow et al., 1988; Wittich, 1991). Within the PBL, the power-law approximations based on the field experiments over Great Plains of the USA, $f_\tau(\zeta) = (1-\zeta)^{3/2}$ and $f_{F_\theta}(\zeta) = 1-\zeta$, are quantitatively quite close to the exponential approximations: $f_\tau(\zeta) = \exp(-\frac{8}{3}\zeta^2)$ and $f_{F_\theta}(\zeta) = \exp(-2\zeta^2)$, which better fit LES data in Figure 1.

It follows that the ratio L/L_N and therefore the role of L_N is small in the upper part of the PBL and increase towards the surface. In other words, the role of the scale L_N is most pronounced in the surface layer. This non-trivial conclusion is consistent with analysis of data from observations in presumably long-lived stable PBLs over Greenland (Zilitinkevich and Calanca, 2000) and Antarctica (Sodemann and Foken, 2004). New LES data shown in Figures 2 and 5 strongly support this conclusion.

It is worth emphasising that our derivation of the resistance and heat-transfer laws is based on the assumption that the ratios τ/u_*^2 and F_θ/F_{θ_s} are universal functions of ζ , but concrete forms of these functions are not required.

Accounting for the alternative limits, L , L_N and L_f , generalised turbulent length scales, $L_{\{M,H\}}$, can be determined through the interpolation:

$$\begin{aligned} \frac{1}{L_{\{M,H\}}} &= \left[\left(\frac{1}{L} \right)^2 + \left(\frac{C_{\{NM,NH\}}}{L_N} \right)^2 + \left(\frac{C_{\{fM,fH\}}}{L_f} \right)^2 \right]^{1/2} \\ &= \frac{1}{L} \left[1 + C_{\{NM,NH\}}^2 \left(\frac{L}{L_N} \right)^2 + C_{\{fM,fH\}}^2 \left(\frac{L}{L_f} \right)^2 \right]^{1/2}, \end{aligned} \quad (14)$$

which gives priority to the smaller scales. Dimensionless coefficients $C_{\{NM,NH\}}$ and $C_{\{fM,fH\}}$ can be different for the turbulent transports of momentum (M) and heat (H).

Recall that the scale L_N was already applied to measure the PBL depth (Kitaigorodskii and Joffre, 1988) and to generalise the Monin-Obukhov similarity theory for the surface layer (Zilitinkevich and Calanca, 2000; Zilitinkevich, 2002). The inverse quadratic interpolation between $L_s \equiv L|_{z=0}$ and L_N was employed to derive an advanced PBL depth model (Zilitinkevich et al., 2002; Zilitinkevich and Baklanov, 2002; Zilitinkevich and Esau, 2002, 2003).

Now, using the composite scale L_M instead of L and matching the log layer in close vicinity of the surface and the z -less stratification layer aloft, the familiar velocity gradient formulation becomes

$$\frac{\partial u}{\partial z} = \frac{\tau^{1/2}}{kz} \left(1 + C_u \frac{z}{L_M} \right) \approx \frac{C_u \tau^{1/2}}{kL_M}, \quad (15)$$

where C_u is a dimensionless constant. Recall that the “ z -less stratification layer” is the height interval within the stably stratified turbulent flow, in which the vertical size of turbulent eddies is controlled by negative buoyancy forces rather than the distance from the surface. Equation (15) differs from the Nieuwstadt (1984) formulation only due to the difference between L_M and L .

Eq. (15) affords an analytical expression of the eddy-viscosity:

$$K_M = \frac{\tau}{\partial u / \partial z} = k \tau^{1/2} z \left(1 + C_u \frac{z}{L_M} \right)^{-1} \approx k C_u^{-1} \tau^{1/2} L_M. \quad (16)$$

Its approximate version, $K_M \approx k C_u^{-1} \tau^{1/2} L_M$, corresponds to the z -less stratification layer ($z \gg C_u^{-1} L$). Principally similar formulations for the potential temperature gradient $\partial \theta / \partial z$ and the eddy conductivity K_M are derived in Section 2.4.

In the surface layer (at $z < 10^{-1} h$), substituting u_* for $\tau^{1/2}$ and $F_{\theta s}$ for F_θ (then $L_M \rightarrow L_{Ms}$), and neglecting the effects of the free flow stability and Earth’s rotation by taking $C_{NM}, C_{fM} = 0$ (then $L_{Ms} = L_s$), Eqs. (15) and (16) reduce to the traditional Monin-Obukhov similarity theory formulation. The latter was verified against experimental data in numerous papers, which gave estimates of C_u in the interval $2 < C_u < 3$. As evident from Eq. (14), this uncertainty can, at least partially, be caused by the difference between L_s and L_{Ms} , and – in shallow PBLs – by unnoticed use of data beyond the surface layer. Indeed, factual length scales L and L_M decrease with increasing height (see Figure 1), which inevitably leads to artificial overestimation of the coefficient C_u if data analysis is based on the traditional, depth-constant Monin-Obukhov length scale L_s .

Eq. (15) is applied to the absolute value of the wind speed $|\mathbf{u}| = (u^2 + v^2)^{1/2}$ rather than to its longitudinal component u (aligned with the turbulent stress at the very surface). The contribution to $|\mathbf{u}|$ from the transverse component v caused by the Coriolis force is small in the surface layer but becomes significant above it.

Figure 2 shows the dimensionless velocity gradient $\Phi_M = \frac{kz}{\tau^{1/2}} \frac{\partial u}{\partial z}$ as dependent on the two versions of the dimensionless height, z/L in Figure 2a and z/L_M in Figure 2b,

and include LES data from the entire PBL. It is seen that the generalised length scale L_M (employed in Figure 2b) provides uniform representation of the three different types of the stable PBL (conventionally neutral, nocturnal and long-lived), and by this means leads to a better collapse of LES data than the traditional scale L . Moreover, this Figure confirms applicability of Eq. (15) throughout the PBL and gives quite certain estimates of empirical constants: $k=0.47$, $C_u=2.5$ and $C_{NM}=0.1$.

To derive a general form of the resistance law, we begin with the nocturnal PBL ($N=0$ and $L_f \gg L$, so that $L_M = L$), then consider the conventionally neutral PBL ($\beta F_{\theta_s} = 0$ and $L_f \gg L$, so that $L_M = L_N$), and the truly neutral PBL ($N = 0$ and $\beta F_{\theta_s} = 0$, so that $L_M = L_f$), and finally interpolate between the resistance laws inherent to these three types of the PBL.

2.2. RESISTANCE LAW FOR NOCTURNAL PBLs

In the surface layer ($z < 10^{-1}h$) within the barotropic nocturnal PBL ($\Gamma = 0$, $N = 0$, $L_f \gg L$), taking $\tau^{1/2} = u_*$ and $L = L_s$, Eq. (15) yields the following expressions for the longitudinal velocity component u :

$$\frac{\partial u}{\partial z} = \frac{u_*}{kz} \left(1 + C_u \frac{z}{L_s} \right) \approx \begin{cases} \frac{u_*}{kz} & \text{at } z \leq C_u^{-1} L_s \\ \frac{C_u u_*}{kL_s} & \text{at } z \geq C_u^{-1} L_s, \end{cases} \quad (17)$$

$$u \approx \begin{cases} \frac{u_*}{k} \ln \frac{z}{z_{0u}} & \text{at } z \leq C_u^{-1} L_s \\ \frac{u_*}{k} \left(\ln \frac{L_s}{C_u z_{0u}} + C_u \frac{z}{L_s} - 1 \right) & \text{at } z \geq C_u^{-1} L_s. \end{cases} \quad (18)$$

Assuming that the vertical profiles of turbulent fluxes are self-similar, Eqs. (13) and (15) in the z -less stratification layer yield $\partial u / \partial z = k^{-1} C_u u_* L_s^{-1} f_u(\zeta)$, where $f_u(\zeta) = f_{F\theta} f_\tau^{-1}$. Then, to account for the effect of baroclinicity, we simply add the baroclinic wind shear Γ_u :

$$\frac{\partial u}{\partial z} = \frac{C_u u_*}{kL_s} f_u(\zeta) + \Gamma_u. \quad (19)$$

This additional term ensures the required upper boundary condition $\partial u / \partial z \rightarrow \Gamma_u$, whereas in the surface layer the term Γ_u is practically negligible compared to the main term (see Appendix in Zilitinkevich and Esau, 2003). Integrating Eq. (19) over z from an arbitrary height z to the PBL upper boundary $z=h$ yields

$$u(h) - u(z) = \frac{C_u u_* h}{k L_s} \Phi_u(\zeta) + \Gamma_u h (1 - \zeta). \quad (20)$$

Here, the function Φ_u is defined as $\Phi_u = \int_{\zeta}^1 f_u(\zeta) d\zeta$, and $u(h) = u_{gh}$ is the u -component of the geostrophic wind at the PBL upper boundary. The latter consists of the barotropic and baroclinic parts:

$$u(h) = u_{g0} + \Gamma_u h = G \cos \alpha + \Gamma_u h, \quad (21)$$

where G and α are the surface values of the geostrophic wind speed and the cross-isobaric angle. Substituting Eq. (21) for $u(h)$ in Eq. (20) yields the longitudinal velocity defect function:

$$G \cos \alpha - u(z) = \frac{C_u u_* h}{k L_s} \Phi_u(\zeta) - \Gamma_u h \zeta, \quad (22)$$

which is valid in the height interval $L_s/h < \zeta < 1$.

Consider Eq. (22) in the z -less stratification part of the surface layer: $L_s/h < \zeta \ll 1$. Here, the term $\Gamma_u h \zeta$ is negligible because $\zeta \ll 1$. Then substituting the lower line on the r.h.s. of Eq. (18) for $u(z)$ yields

$$k \frac{G \cos \alpha}{u_*} - \ln \frac{L_s}{C_u z_{0u}} + 1 = C_u \frac{h}{L_s} [\zeta + \Phi_u(\zeta)] \equiv a \frac{h}{L_s} \quad (a = \text{constant}). \quad (23)$$

The left hand side of Eq. (23) does not depend on ζ . Thus, in the overlapping region, the combination $C_u [\zeta + \Phi_u(\zeta)]$ on the right hand side must be a dimensionless constant (assigned a). Rearranging the terms in Eq. (23) yields the resistance law Equation (7a) with the following A -coefficient:

$$A = -a \frac{h}{L_s} + \ln \frac{h}{L_s} + \ln C_u + 1 = -a \frac{h}{L_s} + \ln \frac{h}{L_s} + \text{constant}, \quad (24)$$

which holds true asymptotically at $h/L_s \gg 1$.

To determine the transverse velocity component, v , consider the Ekman equations:

$$f(v - v_g) + \frac{\partial \tau_x}{\partial z} = 0, \quad -f(u - u_g) + \frac{\partial \tau_y}{\partial z} = 0. \quad (25)$$

Here, τ_x and τ_y are the components of the vertical flux of momentum along the horizontal axes x and y . The x -axis is aligned with the surface stress to make $\tau_y = 0$ at $z = 0$. Hence the boundary conditions are

$$u, v = 0, \tau_x = u_*^2, \tau_y = 0 \text{ at } z = 0; \quad u \rightarrow u_g, v \rightarrow v_g, \tau_x, \tau_y \rightarrow 0 \text{ at } z \rightarrow \infty. \quad (26)$$

Limiting our analysis to the z -less stratification part of the surface layer, we take $u(z)$ from the lower line on the r.h.s. of Eq. (18) and $u_g = G \cos \alpha$ from Eq. (23). This gives the longitudinal velocity-defect function:

$$u - u_g \approx \frac{C_u u_*}{k} \frac{h}{L_s} \left(\zeta - \frac{a}{C_u} \right). \quad (27)$$

Then substituting Eq. (27) for $u - u_g$ in Eq. (25b), integrating over z and accounting for the boundary condition $\tau_y|_{z=0} = 0$ gives the transverse component of the momentum flux:

$$\tau_y = -\frac{afu_*h}{k} \frac{h}{L_s} \left(\zeta - \frac{C_u}{2a} \zeta^2 \right) \approx -\frac{afu_*h}{k} \frac{h}{L_s} \zeta. \quad (28)$$

In the surface layer, the longitudinal component of this flux can be taken depth-constant: $\tau_x \approx \tau_x|_{z=0} = u_*^2$. Then Eq. (16) for the eddy viscosity reduces to

$$K_M = ku_*z \left(1 + C_u \frac{z}{L_s} \right)^{-1}. \quad (29)$$

Next, $\partial v / \partial z$ and v are determined:

$$\frac{\partial v}{\partial z} = \frac{\tau_y}{K_M} = -\frac{af}{k^2} \frac{h}{L_s} \left(1 + C_u \frac{z}{L_s} \right) \approx -\frac{C_u a}{k^2} \left(\frac{h}{L_s} \right)^2 f \zeta, \quad (30)$$

$$v \approx -\frac{C_u a}{2k^2} \left(\frac{h}{L_s} \right)^2 fh \zeta^2, \quad (31)$$

where approximate expressions (\approx) correspond to the z -less stratification part of the surface layer.

To extend the surface-layer formulation Eq. (30) to the upper portion of the PBL, we substitute $L(z)$ for L_s and add to the r.h.s. the baroclinic wind shear Γ_v :

$$\frac{\partial v}{\partial z} = -\frac{C_u a}{k^2} \left(\frac{h}{L_s} \right)^2 f \zeta f_v(\zeta) + \Gamma_v, \quad (32)$$

where $f_v = f_{F\theta}^2 f_\tau^{-3}$ [recall similar reasoning used in the derivation of Eq. (19)].

Integrating Eq. (32) over z from z to h yields

$$v(h) - v(z) = -\frac{C_u a}{k^2} \left(\frac{h}{L_s} \right)^2 fh\Phi_v(\zeta) + \Gamma_v h(1 - \zeta). \quad (33)$$

Here, $\Phi_v = \int_{\zeta}^1 f_v(\zeta) \zeta d\zeta$ is a universal function of ζ , and $v(h) = v_{gh}$ is the v -component of the geostrophic wind at the PBL upper boundary, which consists of the barotropic and baroclinic parts:

$$v(h) = v_{g0} + \Gamma_v h = G \sin \alpha + \Gamma_v h. \quad (34)$$

Substituting Eq. (34) for $v(h)$ in Eq. (33) yields the transverse velocity defect function:

$$G \sin \alpha - v(z) = -\frac{C_u a}{k^2} \left(\frac{h}{L_s} \right)^2 fh\Phi_v(\zeta) - \Gamma_v h\zeta, \quad (35)$$

valid in the height interval $L/h_s < \zeta < 1$. In the z -less stratification part of the surface layer, substituting Eq. (31) for $v(z)$ and neglecting the term $\Gamma_v h\zeta$, Eq. (35) reduces to

$$k \frac{G \sin \alpha}{u_*} = -\frac{C_u a}{2k} \left(\frac{h}{L_s} \right)^2 \frac{fh}{u_*} [\zeta^2 + 2\Phi_v(\zeta)] \equiv -b \frac{fh}{u_*} \left(\frac{h}{L_s} \right)^2 \quad (b = \text{constant}). \quad (36)$$

Here, the combination $C_u a(2k)^{-1} [\zeta^2 + 2\Phi_v(\zeta)]$ turns into a universal dimensionless constant (assigned b) because the left hand side of Eqs. (36) does not depend on ζ . Eq. (36) is nothing but the resistance law Equation (7b) with the resistance-law coefficient

$$B = b \left(\frac{h}{L_s} \right)^2. \quad (37)$$

Likewise Eq. (24), this expression holds true asymptotically at $h/L_s \gg 1$.

In the barotropic steady state, the nocturnal PBL depth becomes $h_E = C_S(L_s u_* / |f|)$, where $C_S \approx 1$ (e.g., Zilitinkevich and Esau, 2003); so the dimensionless parameter in Eqs. (35)-(37) becomes $h/L_s = C_S \mu^{1/2}$, where μ is the traditional internal stability parameter, Eq. (6).

Recall that the very concept of the nocturnal PBL (that is the stable PBL with zero static stability in the free flow: $N=0$) loses its sense in the baroclinic atmosphere. Indeed in the case that $N=0$ but $\Gamma > 0$ the shear-generated turbulence would appear throughout the troposphere.

2.3. EXTENSION OF THE THEORY TO OTHER TYPES OF PBLs

The above analysis is immediately applicable to the conventionally neutral PBL with the only principal difference that the local Monin-Obukhov length scale $L(z)$, Eq. (12a), and its surface value $L_s = -u_*^3(\beta F_{\theta s})^{-1}$ are both substituted by the depth-constant length scale $C_{NM}^{-1} L_N$, where C_{NM} is a dimensionless constant (after Figure 2, $C_{NM} = 0.1$). Thus in the conventionally neutral PBL, the vertical gradients of the velocity components are expressed by formulas similar to Eqs. (19) and (32) but based on the length scale L_N :

$$\frac{\partial u}{\partial z} = \frac{C_u C_{NM} u_*}{k L_N} f_{uN}(\zeta) + \Gamma_u, \quad \frac{\partial v}{\partial z} = -\frac{C_u C_{NM}^2 a}{k^2} \left(\frac{h}{L_N}\right)^2 f_{vN}(\zeta) + \Gamma_v, \quad (38)$$

with the correction functions $f_{uN}(\zeta)$ and $f_{vN}(\zeta)$ different from the functions $f_u(\zeta) = f_{F\theta}(\zeta) f_\tau^{-1}(\zeta)$ and $f_v(\zeta) = f_{F\theta}^2(\zeta) f_\tau^{-3}(\zeta)$ that appeared in Eq. (19) and (32). It follows that the resistance law Equations (7) hold true, but the coefficients A and B become functions of h/L_N :

$$A = -a_N \frac{C_{NM} h}{L_N} + \ln \frac{C_{NM} h}{L_N} + \text{constant}, \quad B = b_N \left(\frac{C_{NM} h}{L_N}\right)^2 \quad (39)$$

with the dimensionless constants a_N and b_N different from a and b . Equations (39) hold true asymptotically at $C_{NM} h/L_N \gg 1$.

In the barotropic steady state, the conventionally neutral PBL depth becomes $h_E = C_C u_* (|f|N)^{1/2}$, where $C_C \approx 1.3$ (see Zilitinkevich and Esau, 2003); so the dimensionless parameter in Eq. (39) becomes $h/L_N = C_C \mu_N^{1/2}$, where μ_N is the external stability parameter, Eq. (10a). This result holds true also in the baroclinic regime, when $h_E = C_C u_T (|f|N)^{1/2}$ and $L_N = u_T / N$. Thus the effect of baroclinicity on the resistance-law coefficients manifests itself only through the dependence of h on the parameter of baroclinicity μ_T , Eq. (10b).

To link the alternative resistance-law formulations Eqs. (24),(37) – for the nocturnal PBL, and Eq. (39a,b) – for the conventionally neutral PBL, we employ the same as in Eq. (14) inverse quadratic interpolation between the turbulent length scales. This yields

$$A = -am_A + \ln m_A + \text{constant}, \quad B = bm_B^2, \quad (40)$$

where m_A and m_B are composite stratification parameters:

$$m_A = \left[\left(\frac{h}{L_s} \right)^2 + \left(\frac{C_{NA} h}{L_N} \right)^2 \right]^{1/2} = \frac{h}{L_s} \left[1 + (C_{NA} \text{Fi})^2 \right]^{1/2}, \quad (41)$$

$$m_B = \left[\left(\frac{h}{L_s} \right)^2 + \left(\frac{C_{NB} h}{L_N} \right)^2 \right]^{1/2} = \frac{h}{L_s} \left[1 + (C_{NB} \text{Fi})^2 \right]^{1/2}. \quad (42)$$

Here, $C_{NA} = C_{NM} a_N a^{-1}$ and $C_{NB} = C_{NM} b_N b^{-1}$ are dimensionless constants, $L_s = -u_*^3 (\beta F_{\text{ob}})^{-1}$ is the Monin-Obukhov length, and $\text{Fi} = N L_s u_*^{-1}$ is an inverse Froude number – already introduced in a generalised surface-layer scaling (Zilitinkevich and Calanca, 2000; Zilitinkevich, 2002).

Finally, in the truly neutral stratification ($\Gamma, N, \beta F_{\text{ob}}, h/L_s, h/L_N, m_A, m_B \rightarrow 0$), taking $h = h_E \sim L_f = u_* / |f|$, the resistance law coefficients $A = A(m_A)$ and $B = B(m_B)$ become universal constants:

$$A(0) = A_0, \quad B(0) = B_0. \quad (43)$$

As already mentioned, the Rossby-Montgomery formula for the truly neutral PBL depth: $h_E = C_R u_* / |f|$ is very well confirmed by LES and lab-experiment data, which give $C_R = 0.7$. The effect of baroclinicity is not relevant to this regime because the baroclinic shear ($\Gamma > 0$) on the background of the neutral static stability ($N=0$) would inevitably result in the appearance of developed turbulence throughout the troposphere.

A reasonable interpolation linking Eq. (40) with Eq. (43) is

$$A = -a m_A + \ln(e^{A_0} + m_A), \quad B = B_0 + b m_B^2. \quad (44)$$

LES data shown in Figures 3 and 4 confirm Eqs. (44) and give estimates of the dimensionless constants $a = 1.4$, $A_0 = 0.5$, $C_{NA} = 0.09$; $b = 10$, $B_0 = 1.5$, $C_{NB} = 0.15$.

The theoretical dependence shown in Figure 4 is nothing but the interpolation between the two asymptotes: $B \rightarrow B_0$ at $m_B \rightarrow 0$ and $B \rightarrow b m_B^2$ at $m_B \rightarrow \infty$ (factually applicable already at $m_B > 2$). Hence, for practical purposes the form of the function $B(m_B)$ in the intermediate interval $0 < m_B < 2$ can be corrected without any violation of the theory.

Recall that the traditional approach did not distinguish between the truly neutral and the conventionally neutral PBLs. Accordingly, in the traditional format (with $m_A = h/L_s$), all data representing different conventionally neutral PBLs would correspond to $h/L_s = 0$, thus causing considerable spread of data points (cf. Figures 10 and 11).

Equations (7), (41)-(42), (44) comprise the resistance law covering a range of neutral and stable PBL regimes, including long-lived stable PBLs, in which both scales L and L_N play important roles, and baroclinic PBLs.

In this context, h is considered as a given parameter. In the steady state, it is equal to the equilibrium stable PBL depth, $h=h_E$, controlled by the three dimensionless parameters: μ , μ_N and μ_Γ (Zilitinkevich and Esau, 2003). Thus our formulation accounts for the effect of baroclinicity on the resistance law coefficients A and B through the dependence of h_E on μ_Γ , Eq. (10). In non-steady regimes, h can be calculated using prognostic relaxation-type equation: $dh/dt \sim t_*^{-1}(h_E - h)$, where $t_* \sim h/u_*$ is the PBL relaxation time scale (see Section 3.2 in Zilitinkevich and Baklanov, 2002).

2.4. PROPER PBL AND CAPPING INVERSION

Notice that stable PBLs experience persistent cooling due to the negative (downward) heat flux at the surface $F_{\theta_s} = F_\theta|_{z=0} < 0$. This cooling results in rising of the capping temperature inversion at the PBL upper boundary. Hence the temperature profile inevitably changes its shape in the course of time and the steady state is never achieved. At the same time, numerous experimental studies convincingly demonstrate that the temperature profile in the surface layer (at $z < 0.1h$) is at least approximately self-similar.

It looks reasonable to assume that the non-stationary changes are basically related to the capping inversion, whereas the temperature profile in the proper PBL shifts quasi-stationary, keeping it self-similar shape. This approach allows considering separately the two mechanisms of essentially different nature:

- maintaining of a self-similar temperature profile in the proper PBL, controlled by instantaneous values of the turbulent fluxes of temperature and momentum and the free-flow Brunt-Väisälä frequency,
- rising of the capping inversion and strengthening of the temperature increment $\Delta\theta_{CI}$ across it.

In the present paper we focus on the heat transfer law for the proper PBL. Recall that the potential temperature in the free atmosphere (outside the PBL) is specified as a linear function of height: $\theta = \theta_{00} + \beta^{-1}N^2z$. Then, given the PBL depth h , the basic-state potential temperature at the PBL upper boundary is an easily determined external parameter⁴:

$$\theta_{h+0} \equiv \theta_{00} + \frac{N^2}{\beta}h, \quad (45)$$

⁴ In our LES, θ_{00} is nothing but the initial value of θ at the surface: $\theta_{00} = \theta|_{z=0, t=0}$.

To distinguish between the proper PBL and the capping inversion, we determine the inversion half-depth, $\frac{1}{2}\delta_{CI}$, as the height interval between the PBL upper boundary, $z=h$, and the inflection point just below this level, that is the height $z = h - \frac{1}{2}\delta_{CI}$, at which $\partial\theta/\partial z$ approaches minimum ($\partial^2\theta/\partial z^2=0$) and start increasing (then no inflection point means no capping inversion). Considering the potential temperature at this height, $\theta_{h-0} \equiv \theta|_{z=h-\frac{1}{2}\delta_{CI}}$, as a reference value of θ at the upper boundary of the proper PBL, the potential temperature increment across the capping inversion, $\Delta\theta_{CI}$, is defined as

$$\Delta\theta_{CI} = \theta_{h+0} - \theta_{h-0}. \quad (46)$$

As already mentioned we leave determining $\Delta\theta_{CI}$ for a separate paper and limit our analysis to the derivation of the heat transfer law for the proper PBL in terms of the potential temperature increment across the PBL:

$$\Delta\theta_{PBL} = \theta_{h-0} - \theta_0. \quad (47)$$

Clearly, in the PBLs with no capping inversions (e.g., in the nocturnal PBLs), this definition reduces to the traditional one: $\Delta\theta_{PBL} = \theta_h - \theta_0 = \theta_{h+0} - \theta_0$.

Consider the similarity-theory formulation for the potential temperature gradient:

$$\frac{\partial\theta}{\partial z} = \frac{\theta_*}{k_T z} \left(1 + \frac{C_\theta z}{L_H} \right) \quad (48)$$

based on the traditional turbulent temperature scale $\theta_* = -F_\theta\tau^{-1/2}$ and the generalised z -dependent turbulent length scale L_H , Eq. (14). Eq. (48) is derived similarly to Eq. (15) through matching the temperature-gradient scales θ_*/z and θ_*/L_H for the log-layer and the z -less stratification layer, respectively.

Figure 5 shows LES data on $\Phi_H = \frac{k_T z}{\theta_*} \frac{\partial\theta}{\partial z}$ as dependent on either z/L (Figure 5a) or z/L_H (Figure 5b) in the height interval $0 < z < h - \frac{1}{2}\delta_{CI}$ for the nocturnal (x) and long-lived (o) stable PBLs⁵. It confirms applicability of Eq. (48) throughout the proper PBL and demonstrates that the generalised scaling provides reasonably good collapse of practically all LES data taking the following values of dimensionless constants: $k_T=0.47$, $C_\theta = 2$ and $C_{NH} = 1.5$. In other words, the scale L_H is applicable to both nocturnal and long-lived PBLs in contrast to the traditional scale L applicable only to the nocturnal PBLs.

⁵ In the conventionally neutral PBLs the potential temperature flux approaches zero at the surface: $F_\theta|_{z=0} = 0$. Hence, the temperature scale θ_* is inappropriate and data representing these PBLs cannot be shown in Figure 5.

Recalling the turbulent-flux profile approximations (given in Figure 1), Figure 5 supports an analytical eddy-conductivity formulation⁶:

$$K_H = \frac{-F_\theta}{\partial\theta/\partial z} = k_T \tau^{1/2} z \left(1 + C_\theta \frac{z}{L_H} \right)^{-1} \approx k_T C_\theta^{-1} \tau^{1/2} L_H, \quad (49)$$

where approximate expression (\approx) corresponds to the z -less stratification layer ($z \gg C_\theta^{-1} L$).

In further analysis we exclude the capping inversion layer and derive the heat transfer law for the proper PBL.

2.5. HEAT TRANSFER LAW

Consider first the nocturnal PBL. In the surface layer within this PBL, Eq. (48) yields

$$\frac{\partial\theta}{\partial z} = \frac{\theta_{*s}}{k_T z} \left(1 + C_\theta \frac{z}{L_s} \right) \approx \begin{cases} \frac{\theta_{*s}}{k_T z} & \text{at } z \leq C_\theta^{-1} L_s \\ \frac{C_\theta \theta_{*s}}{k_T L_s} & \text{at } z \geq C_\theta^{-1} L_s, \end{cases} \quad (50)$$

$$\theta - \theta_0 \approx \begin{cases} \frac{\theta_{*s}}{k_T} \ln \frac{z}{z_{0u}} & \text{at } z \leq C_\theta^{-1} L_s \\ \frac{\theta_{*s}}{k_T} \left(\ln \frac{L_s}{C_\theta z_{0u}} + C_\theta \frac{z}{L_s} - 1 \right) & \text{at } z \geq C_\theta^{-1} L_s. \end{cases} \quad (51)$$

In the z -less stratification part of the PBL [at $L(z) \ll z < h$], accounting for the self-similarity of the normalised turbulent fluxes, $\tau / u_*^2 = f_\tau(\zeta)$ and $F_\theta / F_{\theta s} = f_{F\theta}(\zeta)$, and employing the formula $\theta_*(z) \approx \theta_{*s}$ (see Figure 1), Eq (48) reduces to

$$\frac{\partial\theta}{\partial z} = \frac{C_\theta \theta_{*s}}{k_T L_s} f_\theta(\zeta), \quad (52)$$

where $f_\theta = f_{F\theta}^2 f_\tau^2 \rightarrow 1$ at $\zeta \rightarrow 0$. Integrating Eq. (52) from z to $h - \frac{1}{2} \delta_{Cl}$ yields the potential-temperature defect function:

$$\theta_{h-0} - \theta(z) = \frac{C_\theta (h - \frac{1}{2} \delta_{Cl}) \theta_{*s}}{k_T L_s} \Phi_\theta(\zeta) \approx \frac{C_\theta h \theta_{*s}}{k_T L_s} \Phi_\theta(\zeta), \quad (53)$$

⁶ Similar scaling reasoning in combination with analysis of LES data could be applied to derive a simple analytical formulation for the eddy diffusivity. Such a formulation could be useful in pollution dispersion modelling, especially in strong static stability regimes, when traditional formulations often give poor results.

where $\Phi_\theta = \int_\zeta^1 f_\theta(\zeta) d\zeta$. The approximate expression on the r.h.s. of Eq. (53) is justified when the capping inversion layer is comparatively shallow: $\frac{1}{2}\delta_{CI} \ll h$.

Considering Eq. (53) in the z -less stratification part of the surface layer and substituting the lower line of Eq. (51) for $\theta(z)$ on the l.h.s. of Eq. (53) yields

$$k_T \frac{\theta_{h-0} - \theta_0}{\theta_{*s}} - \ln \frac{L_s}{C_\theta z_{0u}} - 1 = C_\theta \frac{h}{L_s} [\zeta + \Phi_\theta(\zeta)] = c \frac{h}{L_s} \quad (c = \text{constant}). \quad (54)$$

The r.h.s. of Eq. (54) is nothing but universal constant (assigned c) because the l.h.s. of this Equation does not depend on z .

Eq. (54) is consistent with the temperature resistance law Eq. (8) [provided that the temperature increment across the PBL is defined after Eq. (47)] and implies the following asymptotic expression of the C -coefficient at $h/L_s \gg 1$:

$$C = -c \frac{h}{L_s} + \ln \frac{h}{L_s} + \ln C_\theta + 1 = -c \frac{h}{L_s} + \ln \frac{h}{L_s} + \text{constant}. \quad (55)$$

Employing the same approach as in Section 2.3, Eq. (55) is immediately extended to include both the near-neutral and the long-lived stable PBLs:

$$C = -cm_C + \ln(e^{C_0} + m_C) \approx -cm_C + C_0, \quad (56)$$

where m_C is a composite stratification parameter:

$$m_C = \left[\left(\frac{h}{L_s} \right)^2 + \left(\frac{C_{NC} h}{L_N} \right)^2 \right]^{1/2} = \frac{h}{L_s} [1 + (C_{NC} \text{Fi})^2]^{1/2}, \quad (57)$$

and $C_0 = C(0)$ is the limiting value of the coefficient C in the near-neutral stratification (when $m_C \ll 1$).

Recall that the baroclinic versions of the turbulent length scale and the equilibrium PBL depth are $L_N = u_T / N$, and $h_E \sim u_T (|f|/N)^{-1/2}$, where u_T is given by Eq. (11). Hence the effect of baroclinicity on the ratio h/L_N can be neglected, at least as a first approximation [cf. the same conclusion in the discussion of Eq. (39) and in the very end of Section 2.3].

Equations (5), (8), (12), (56) and (57) comprise the heat transfer law. LES data shown in Figure 6 confirm Eqs. (56), (57) with reasonable accuracy and give estimates of the dimensionless constants $C_{NC} = 1.2$, $c = 4.1$ and $C_0 = 12$. Quite large value of C_0 justifies the approximate version of Eq. (56).

3. Large-eddy simulations

In this paper we systematically use data from numerical simulations based on a new LES code (Esau, 2004a). This code solves the momentum, temperature and continuity equations for incompressible Boussinesq fluid:

$$\frac{\partial u_i}{\partial t} = -\frac{1}{2}u_j \frac{\partial u_i}{\partial x_j} - \frac{\partial}{\partial x_j} \left(\frac{1}{2}u_i u_j + p\delta_{ij} + \tau_{ij} \right) - f\omega_j - \frac{g}{T_0}\Theta\delta_{i3}, \quad (58)$$

and

$$\frac{\partial \Theta}{\partial t} = -\frac{\partial}{\partial x_j} (u_j \Theta + \tau_{\Theta j}), \quad \frac{\partial u_i}{\partial x_i} = 0 \quad (59)$$

Here, $u_i = \{u, v, w\}$, Θ , p are large scale velocity, potential temperature and pressure; τ_{ij} , $\tau_{\Theta j}$ are sub-grid scale turbulence stress and diffusivity tensors; $f\omega_j = \{f(v_g - v - w \cdot \cot \varphi), f(-u_g + u), fu \cdot \cot \varphi\}$ are the components of the Coriolis force; f is the Coriolis parameter; φ is the latitude; $\delta_{ij} = 1$ at $i = j$ and $\delta_{ij} = 0$ and $i \neq j$; the repeating indexes imply summation.

The code uses the fully conservative second order central difference scheme (Morinishi *et al.*, 1998) for advection and the fourth order Runge-Kutta scheme (Jameson *et al.*, 1981) for time stepping. The direct fractional-step pressure correction scheme (Armfield and Street, 1999) ensures incompressibility in the code. This set of numerical schemes is a kind of standard in computational fluid dynamics. Moreover, Andren *et al.* (1994) concluded that differences in numerical schemes have a minor effect on LES results. Later, Brown *et al.* (2000) reported that LES results are encouragingly insensitive to the choice of numerical schemes, as long as simulations resolve some part of the inertial sub-range of scales. The computational mesh is the staggered C-type mesh. The grid spacing is uniform and almost isotropic. The horizontal grid size Δ_x is larger than the vertical grid size Δ_z , but their ratio Δ_x/Δ_z is always less than four.

An important part of the LES technique is a sub-grid turbulence closure. This LES code employs a dynamic mixed closure (Vreman *et al.*, 1994):

$$\tau_{ij} = \left[\overline{(u_i u_j)} - \overline{(u_i)} \overline{(u_j)} \right] + \left[-2l_s^2 |S_{ij}| S_{ij} \right], \quad S_{ij} = \frac{1}{2} \left(\frac{\partial u_i}{\partial x_j} + \frac{\partial u_j}{\partial x_i} \right), \quad (60)$$

$$\tau_{\Theta j} = -2 \text{Pr}_t^{-1} l_s^2 |S_{ij}| \frac{\partial \Theta}{\partial x_j}, \quad (61)$$

where, Pr_t is an empirical turbulent Prandtl number taken after Kondo *et al.* (1978).

The first term $\left[\overline{(u_i u_j)} - \overline{(u_i)} \overline{(u_j)}\right]$ represents the direct dissipation of energy in non-linear interactions of large eddies. The filter (denoted by overbar) determines the scale interval in which this direct energy dissipation is possible. In the present LES code, the interval has the size of two grid cells. This term was not included in prior environmental LES codes. Its importance has been recognised only recently through analyses of data from the HATS atmospheric field experiment (Sullivan *et al.*, 2003).

The second term $-2l_s^2 |S_{ij}| S_{ij}$ in Eq.(60) and the term $-2Pr_t^{-1} l_s^2 |S_{ij}| \frac{\partial \Theta}{\partial x_j}$ in Eq. (61)

represent a Smagorinsky type of the eddy-viscosity closure (Smagorinsky, 1963). It parameterises local and instant energy dissipation by small eddies through numerical solution of a variation problem for the mixing length scale $l_s(x_i, t)$ at every time step. Comparative tests of this LES code are presented by Esau (2004a).

It is worth mentioning that advantages of the dynamic mixed closure become important only in the case of strong flow anisotropy or very strong static stability. Both cases are actually equivalent since the strong static stability increases the eddy anisotropy. In these cases, the first term in Eq. (60a) becomes large or even dominant. The most of the LES runs in our database correspond to moderate flow anisotropy and static stability, thus, the sub-grid turbulence closure should not be considered as a critical component of the present study.

The design of all LES runs followed a standard scheme. The LES domain had 64 grid points in each direction. Chapman (1978) provided the following criterion of a well-resolved boundary-layer flow: 15-30 computational levels within the PBL. We followed this criterion. The PBL always comprised about 1/2 to 2/3 of the LES domain. Accordingly, the physical resolution varied from about 0.5 m (for very stable PBL runs) to more than 50 m (for truly neutral PBL runs).

Figure 7 shows the quality of the LES in terms of the ratio Q_E of the sub-grid turbulent kinetic energy (TKE) to the resolved TKE: $Q_E = \int_0^h E^{SGS} dz / \int_0^h E^{RES} dz$, presented as dependent on the dimensionless resolution Δ_z / L_* , where Δ_z is the vertical grid size, and L_* is the turbulent length scale. Clearly, both ratios Q_E and Δ_z / L_* should be small in well-resolved LES. Our LES runs satisfied the conditions $Q_E < 1/4$ and $\Delta_z / L_* < 1$, which gives grounds to expect that the sub-grid scale effects were negligible.

The upper boundary conditions are of von Neumann type or stressless rigid lid, $\nabla_z u_i = \nabla_z \Theta = \nabla_z p = 0$, $w = 0$.

The bottom boundary conditions are

- prescribed sub-grid scale turbulent flux of potential temperature $\tau_{\Theta j}$,
- logarithmic wall-law: $\tau_{i3} = (\kappa |u_i(z = \Delta_z / 2)| / \ln(\Delta_z / 2z_0))^2$, $\tau_{i1} = \tau_{i2} = 0$, where $\Delta_z / 2$ is the height of the first computational level.

The initial mean profiles are specified as linearly increasing potential temperature (a prescribed depth-constant temperature gradient) and a prescribed depth-constant wind velocity at all levels down to the surface. The initial flow is laminar with imposed very small random perturbations at the first 3-5 computational levels. The initial profiles, perturbations, surface fluxes and the Coriolis force are not adjusted to each other. Hence every run goes through a spin up phase. During this period (usually 3-5 model hours) all turbulence characteristics are statistically unsteady. As an example, Figures 8 and 9 show the temporal evolution of the A , B and C coefficients in the truly neutral and the long-lived stable PBL runs.

The typical run duration is 64800 s. (18 model hours). We accept that the basic characteristics of turbulence reach the steady state in the last 7 model hours. Averaging over this time interval is used to create the database.

To account for the residual, long-term variations of turbulent characteristics, we (probably for the first time in LES practice) calculated and plotted not only the mean values of the modelled parameters (in particular the A , B and C coefficients) but also their standard deviations. These residual variations are partially caused by incomplete achievement of the steady state. This effect is especially pronounced for such sensitive parameters as the cross-isobaric angle α (therefore the B -coefficient) and the temperature increment across the proper PBL $\Delta\theta_{PBL}$ (therefore the C -coefficient). It causes rather large scatter of data points in Figures 4 and 6. In very stable PBLs, the scatter could also be caused by the turbulence intermittency (Mahrt, 1985).

4. Verification of resistance and heat transfer laws against LES data

Earlier atmospheric measurements gave very uncertain estimates of the \tilde{A} , \tilde{B} and \tilde{C} (or A , B and C) coefficients, considered – according to the theoretical expectations of the time – as single-valued functions of $\mu = u_* / |f| L_s$ (or h/L_s). Although data from one particular field-experiment programme, such as Cabauw (Nieuwstadt, 1981) or Wangara (Yamada, 1976), could show reasonable collapses, data summaries including results from different experimental sites always exhibited enormously huge scatter (e.g., Zilitinkevich and Chalikov, 1968; Zilitinkevich, 1975). Besides insufficient accuracy of earlier experiments, this huge scatter could be to some extent caused by the newly recognised effects, namely the free-flow stability, baroclinicity and deviations from the equilibrium state, overlooked in the prior resistance and heat-transfer formulations.

As illustrations, Figures 10-12 present the \tilde{A} , \tilde{B} and \tilde{C} coefficients in the traditional way – as functions μ , putting together data from earlier atmospheric measurements, earlier LES and new LES database. In this old format, the earlier and the new LES data, although showed reasonably good results in Figures 3, 4 and 6, only added to the scatter. It is not surprising that the old theoretical curves for $\tilde{A}(\mu)$, $\tilde{B}(\mu)$ and $\tilde{C}(\mu)$ taken from Byun (1991) reflect this scatter and look rather chaotic. Unfortunately the earlier atmospheric data did not include sufficient information to present them in the new format. Anyhow, striking difference between Figures 10-12 based on the old theory and Figures 3, 4 and 6 based on the advanced theory catches the eye.

The advantage of new theory is very clearly seen at the weak- and moderate-stability regimes. Indeed, the traditional type of functions $\tilde{A}(\mu)$, $\tilde{B}(\mu)$ and $\tilde{C}(\mu)$ exhibit incomparably larger scatter at small values of the internal stability parameter μ than the new functions $A(m_A)$, $B(m_B)$ and $C(m_C)$ at small values of the composite stability parameters m_A , m_B and m_C . Pronounced scatter of data on $C(m_C)$ at very small m_C is not surprising because small values of m_C imply very small temperature fluxes and temperature increments across the PBL, which inevitably results in considerable errors in the estimates of θ_* , $\Delta\theta_{PBL}$ and m_C .

Probably for the first time, quite certain estimates of A and B are obtained from LES runs for the truly neutral PBL. This allows determining the dimensionless constants $A_0 = A|_{m_A=0}$ and $B_0 = B|_{m_B=0}$ with a reasonably high accuracy. Figures 13 and 14 show all data on A_0 and B_0 from our database versus the surface Rossby number $Ro = G/|f|z_{ou}$. The graphs do not exhibit any dependence on Ro and demonstrate that A_0 and B_0 can be treated as universal constants: $A_0 = 1.9 \pm 0.9$ and $B_0 = 1.5 \pm 0.5$. It is obvious that the constant $C_0 = C|_{m_C \rightarrow 0}$ cannot be deduced in the same way from LES runs for the truly neutral PBLs. Instead, it is determined from the best fit of the theoretical curve $C = -cm_C + \ln(e^{C_0} + m_C)$ to all available LES data, which gives $C_0 = 12$. All dimensionless empirical constants appeared in the new theory are summarised in Table 1.

5. Conclusions

In the traditional context, the terms “stably stratified atmospheric PBL” and “nocturnal PBL” were considered as synonyms, whereas the term “neutrally stratified PBL” was applied to all PBLs characterised by the zero buoyancy flux at the surface ($F_{\theta_s} = 0$) without any regard to the Brunt-Väisälä frequency N in the free atmosphere above the PBL. In contrast, we distinguish between the following essentially different types of the stable PBLs:

- *Short-lived* PBLs, namely, the nocturnal stable ($F_{\theta_s} < 0$, $N = 0$) and the truly neutral ($F_{\theta_s} = 0$, $N = 0$) PBLs that develop against neutrally stratified residual layers. They exhibit basically local nature. In these regimes, the Monin-Obukhov similarity theory realistically describes the surface layer turbulence.
- *Long-lived* PBLs, namely, the thoroughly stable ($F_{\theta_s} < 0$, $N > 0$) and the conventionally neutral ($F_{\theta_s} = 0$, $N > 0$) PBLs that develop during sufficiently long period to approach the stably stratified free atmosphere. Their basic features (including the surface-layer scaling) are essentially controlled by the non-local effect of N . In these regimes, the classical similarity theory is no longer: besides the familiar Monin-Obukhov length scale L , an important role is played by the external stability scale $L_N = u_* / N$.

At $N=0$, the effect of baroclinicity would result in the overall turbulisation of the troposphere. It is not surprising that the traditional short-lived PBL models did not account for this effect. On the contrary, additional mixing due to the baroclinic shear ($\Gamma = |\partial \mathbf{u}_g / \partial z|$) is very naturally included in the long-lived PBL model through the baroclinic turbulent velocity scale $u_T = u_* (1 + C_0 \Gamma / N)^{1/2}$.

In the present paper, the resistance and heat transfer laws are advanced accounting for the effects of the N and Γ disregarded in prior models and now reflected through composite stratification parameters m_A , m_B and m_C , Eq. (41), (42) and (57), and the baroclinic PBL depth formulation (Zilitinkevich and Esau, 2003).

The newly derived resistance-law formulation for the cross-isobaric angle, Eq. (7b), explicitly shows the role of the Coriolis parameter f .

The proposed theory sheds light on the cause of a very wide spread of data in prior empirical graphs presenting the resistance-law coefficients as single-valued functions of a sole stratification parameter, such as $\mu = u_* / |f| L_s$ or h/L_s . It is shown that this spread was to a large extent caused by the effects uncouncted in the traditional context. Analogous graphs based on the new theory exhibit considerable collapse of LES data.

The resistance and heat transfer laws given by Eqs. (5), (7), (8), (41), (42), (44), (56) and (57) provide physical background for an advanced surface-flux calculation scheme applicable to a wide range of PBLs including very shallow boundary layers. Such a scheme would respond to urgent demand from operational modelling. Indeed, all currently used surface-flux schemes are based on the concept of the surface layer, which implies that the turbulent fluxes are taken depth-constant ($\tau = u_*^2$, $F_\theta = F_{\theta_s}$) from the surface $z=0$ up to the lowest computational level $z=z_1$. Clearly, this assumption is justified only when the PBL height h is an order of magnitude larger than z_1 . However, in operational models z_1 cannot be taken too small (in particular, z_1 is close to 30 m in the most advanced numerical weather prediction and climate models ECMWF, HIRLAM and ECHAM). At the same time, as recognised recently, the typical height of long-lived stable PBLs is just a few dozen metres (Zilitinkevich and Esau, 2003). Traditional surface-flux schemes completely fail in such cases (see Esau, 2004b); so the resistance-law based approach simply has no alternative.

New advancement of the resistance and heat-transfer laws makes them principally applicable to the oceanic upper and bottom PBLs. Notice that the role of the external stability parameter μ_N , Eq. (10), is absolutely dominant in the upper layer of water, because of the very strong static stability typically observed in the thermocline below the PBL. It is conceivable that the advanced laws – reformulated and validated against oceanographic data – can be used as the physical basis for improved calculations of the key parameters characterising the oceanic PBLs: turbulent fluxes of momentum and scalars at the ocean bottom; velocity and direction of the surface drift currents; increments in the temperature, salinity and other scalar admixtures across thin films at the water surface (see Zilitinkevich and Kreiman, 1991). Such calculations are required in a number of practical problems, such as modelling of CO₂ exchanges

between the atmosphere and the ocean, modelling of transport and dispersion of oil films at the water surface, etc.

LES data analyses performed here to support our background assumptions and to validate final results (and LES data base as such) could be of interest beyond this research. In particular, they reveal well-pronounced self-similarity of normalised turbulent-flux profiles (Figure 1) and confirm feasibility of the generalised scaling based on Eq. (14) for all kinds of stable PBLs (Figures 2 and 5).

Acknowledgements

The authors thank Dale Hess and Sylvain Joffre for valuable comments. This work has been supported by the EU Marie Curie Chair Project MEXC-CT-2003-509742, ARO Project “Improved Parameterisation of Stably Stratified Boundary Layer Turbulence in Atmospheric Models” – DAAD 19-01-1-0816; EU Project FUMAPEX EVK4-2001-00281, Norwegian project MACESIZ 155945/700, and joint Norwegian-USA project ROLARC 151456/720.

References

- Andren, A., Brown, A.R., Graf, J., Mason, P.J., Moeng, C-H., Nieuwstadt, F.T.N., and Schumann, U., 1994: Large-eddy simulation of a neutrally stratified layer: A comparison of four computer codes. *Quart. J. Roy. Met. Soc.*, **120**, 1457-1484.
- Arya, S.P.S., 1975: Comments on "Similarity theory for the planetary boundary layer of tome-dependent height". *J. Aytmos. Sci.*, **32**, 839-840.
- Arya, S.P.S., and Wyngaard, J.C., 1975: Effect of baroclinicity on wind profiles and the geostrophic drag law for the convective planetary boundary layer. *J. Atmos. Sci.*, **32**, 767-778.
- Armfield, S. and Street, R., 1999: The fractional step method for the Navier-Stokes equations on staggered grids: The accuracy of three variations. *J. Comput. Phys.*, **153**, 660-665.
- Brown, A.R., Derbshire, S.H., and Mason, P.J., 1994: Large-eddy simulation of stable atmospheric boundary layers with a revisited stochastic backscatter subgrid model. *Quart. J. Roy. Met. Soc.*, **120**, 1485-1512.
- Brown, A.R., MacVean, M.K., and Mason, P.J., 2000: The effects of numerical dissipation in large eddy simulations. *J. Atmos. Sci.* **57**, 3337-3348.
- Byun, D., 1991: Determination of similarity functions of the resistance laws for the planetary boundary layer using surface layer similarity functions. *Boundary-Layer Meteorol.*, **57**, 17-48.
- Chapman, D.R., 1978: Computational aerodynamics, development and outlook. *AIAA J.*, **17**(12), 1293-1313.
- Csanady, G. T., 1974: Equilibrium theory of the planetary boundary layer with an inversion lid. *Boundary-layer Meteorol.*, **6**, 63-79.
- Djolov, G., Yordanov, D., and Syrakov, D., 2004: Baroclinic planetary boundary layer model for neutral and stable stratification conditions. *Boundary Layer Meteorol.*, **111**, 467-490.
- Esau, I.N., 2004a: Simulation of Ekman boundary layers by large eddy model with dynamic mixed sub-filter closure, *Env. Fluid Mech.*, **4**, 273-303.
- Esau, I.N., 2004b: Parameterization of a surface drag coefficient in conventionally neutral planetary boundary layer. *Annales Geophysicae.* **22**, 3353-3362.
- Garratt, J. R., 1992: *The Atmospheric Boundary Layer*. Cambridge University Press, 316 pp.
- Gill, A.E., 1968: Similarity theory and geostrophic adjustment. *Quart. J. Roy. Met. Soc.*, **94**, 586-588.
- Hess, G.D., 2004: The neutral, barotropic planetary boundary layer, capped by a low-level inversion, *Boundary-Layer Meteorol.*, **110**, 319-355.
- Hess, G.D. and Garratt, J.R., 2002a: Evaluating models of the neutral, barotropic planetary boundary layer using integral measures: Part I. Overview, *Boundary-Layer Meteorol.*, **104**, 333-358.
- Hess, G.D., and Garratt, J.R., 2002b: Evaluating models of the neutral, barotropic planetary boundary layer using integral measures: Part II. Modelling Observed Conditions, *Boundary-Layer Meteorol.*, **104**, 359-369.
- Jameson, A., Schmidt, W., and Turkel, E. 1981: Numerical simulation of Euler equations by finite 77 volume methods using Runge-Kutta time stepping schemes. *AIAA Paper*, **81**, 1259.
- Joffre, S. M., 1982: Assessment of separate effects of baroclinicity and thermal stability in the atmospheric boundary layer over the sea. *Tellus*, **34**, 567-578.

- Joffre, S. M., 1985: Effects of local accelerations and baroclinicity on the mean structure of the atmospheric boundary layer over the sea. *Boundary-Layer Meteorol.*, **32**, 237-255.
- Kazanski A.B., and Monin, A.S., 1961: On turbulent regime above the surface layer, *Izvestija AN SSSR Geophysical Series*, No. 1, 165-168.
- King, J., and Turner, J., 1997: *Antarctic Meteorology and Climatology*. Cambridge University Press.
- Kitaigorodskii, S. A., and Joffre, S. M., 1988; In search of simple scaling for the heights of the stratified atmospheric boundary layer, *Tellus*, **40A**, 419-43.
- Kondo, J., Konechika, O., and Yasuda, N., 1978: Heat and momentum transfer under strong stability in the atmospheric surface layer. *J. Atmos. Sci.*, **35**, 1012-1021.
- Kosovic, B., and Curry, J., 2000: A large eddy simulation study of a quasi-steady, stably stratified atmospheric boundary layer. *J. Atmos. Sci.*, **57**, 1052-1068.
- Lenschow, D.H., Li, X.S., Zhu, C.J., and Stankov, B.B., 1988: The stably stratified boundary layer over the Great Plains. Part 1: Mean and turbulence structure. *Boundary-layer Meteorol.*, **42**, 95-121.
- Marht, L., 1985: Vertical structure and turbulence in the very stable boundary layer, *J. Atmos. Sci.*, **42**, 2333-2349.
- Mahrt, L. and Vickers, D., 2002: Contrasting vertical structures of nocturnal boundary layers, *Boundary Layer Meteorol.*, **105**, 351-363.
- Mason, P.J., 1994: Large-eddy simulation: A critical review of the technique. *Quart. J. Roy. Met. Soc.*, **120**, 1-26.
- Monin, A.S., and Obukhov, A.M., 1954: Main characteristics of the turbulent mixing in the atmospheric surface layer, *Trudy Geophys. Inst. AN. SSSR*, **24**(151), 153-187.
- Morinishi, Y., Lund, T.S., Vasiljev, O.V., and Moin, P. 1998: Fully conservative higher order finite difference schemes for incompressible flow. *J. Comput. Phys.*, **143**, 90-124.
- Nieuwstadt, F.T.M., 1981: The steady-state height and resistance laws of the nocturnal boundary layer: Theory compared with Cabauw observations. *Boundary-Layer Meteorol.*, **20**, 3-17.
- Nieuwstadt, F.T.M., 1984: The turbulent structure of the stable nocturnal boundary layer. *J. Atmos. Sci.*, **41**, 2202-2216.
- Overland, J. E., and Davidson, K. L., 1992: Geostrophic drag coefficient over sea ice. *Tellus*, **44A**, 54-66.
- Rossby, C.G., and Montgomery, R.B., 1935: The layers of frictional influence in wind and ocean currents, *Pap. Phys. Oceanogr. Meteorol.*, **3**(3), 101 pp.
- Smagorinsky, J., 1963: General circulation experiments with the primitive equations. *Mon. Weather Rev.*, **91**(3), 99-164.
- Sodemann, H., and Foken, T., 2004: Empirical evaluation of an extended similarity theory for the stably stratified atmospheric surface layer. *Quart. J. Roy. Met. Soc.*, **130**, 2665-2671.
- Sorbjan, Z., 1988: Structure of the stably-stratified boundary layer during the SESAME-1979 experiment. *Boundary-Layer Meteorol.*, **44**, 255-266.
- Sullivan, P.P., Horst, Th.W., Lenschow, D.H., Moeng, C.-H., and Weil, J.C.: 2003: Structure of subfilter-scale fluxes in the atmospheric surface layer with application to large-eddy simulation modelling. *J. Fluid Mech.*, **482**, 101-139.
- Tjenstroem, M., and Smedman A.-S., 1993: The vertical structure of the coastal marine atmospheric boundary layer, *J. Geophys. Res.*, **98**(C3), 4809-4826.

- Vreman, B., Geurts, B. and Kuerten, H., 1994: On the formulation of the dynamic mixed subgrid-scale model. *Phys. Fluids*, **6**(12), 4057-4059.
- Wittich, K.P., 1991: The nocturnal boundary layer over Northern Germany: an observational study. *Boundary-Layer Meteorol.*, **55**, 47-66.
- Yamada, T., 1976: On similarity functions A, B and C of the planetary boundary layer, *J. Atmos. Sci.*, **33**, 781-793.
- Zilitinkevich, S.S., Laikhtman, D.L., and Monin, A.S., 1967: Dynamics of the boundary layer in the atmosphere. *Izvestija, AN SSSR, FAO*, **3**, No. 3, 297-333.
- Zilitinkevich, S.S., and Chalikov, D.V., 1968: On the resistance and heat/moisture transfer laws in the interaction between the atmosphere and the underlying surface. *Izvestija AN SSSR, FAO*, **4**, No. 7, 765-772.
- Zilitinkevich, S.S., 1972: On the determination of the height of the Ekman boundary layer. *Boundary-Layer Meteorol.*, **3**, 141-145.
- Zilitinkevich, S.S., and Dearnorff, J.W., 1974: Similarity theory for the planetary boundary layer of time-dependent height. *J. Atmos. Sci.*, **31**, 1449-1452.
- Zilitinkevich, S.S., 1975: Resistance laws and prediction equations for the depth of the planetary boundary layer. *J. Atmos. Sci.*, **32**, 741-752.
- Zilitinkevich, S.S., 1989: Velocity profiles, resistance law and the dissipation rate of mean flow kinetic energy in a neutrally and stably stratified planetary boundary layer, *Boundary-Layer Meteorol.*, **46**, 367-387.
- Zilitinkevich, S.S., and Kreiman, K.D., 1991: Wind-induced drift of surface films. Chapter 4 in "Modelling Air-Lake Interaction. Physical Background" (edited by S.S. Zilitinkevich). Springer-Verlag, Berlin, 63-73.
- Zilitinkevich, S., Johansson, P.-E., Mironov, D.V., and Baklanov, A., 1998b: A similarity-theory model for wind profile and resistance law in stably stratified planetary boundary layers. *J. Wind Eng. Industr. Aerodyn.*, **74-76**, 209-218.
- Zilitinkevich, S., and Calanca, P., 2000: An extended similarity-theory for the stably stratified atmospheric surface layer. *Quart. J. Roy. Meteorol. Soc.*, **126**, 1913-1923.
- Zilitinkevich, S.S., Grachev, A.A., and Fairall, C.W., 2001: Scaling reasoning and field data on the sea-surface roughness lengths for scalars. *J. Atmos. Sci.*, **58**, 320-325.
- Zilitinkevich, S., 2002: Third-order transport due to internal waves and non-local turbulence in the stably stratified surface layer. *Quart. J. Roy. Met. Soc.* **128**, 913-925.
- Zilitinkevich, S.S., and Baklanov, A., 2002: Calculation of the height of stable boundary layers in practical applications. *Boundary-Layer Meteorol.*, **105**, 389-409.
- Zilitinkevich S.S., and Esau, I.N., 2002: On integral measures of the neutral, barotropic planetary boundary layers. *Boundary-Layer Meteorol.*, **104**, 371-379.
- Zilitinkevich, S., Baklanov, A., Rost, J., Smedman, A.-S., Lykosov, V., and Calanca, P., 2002: Diagnostic and prognostic equations for the depth of the stably stratified Ekman boundary layer. *Quart. J. Roy. Met. Soc.*, **128**, 25-46.
- Zilitinkevich S.S., and Esau, I.N., 2003: The effect of baroclinicity on the depth of neutral and stable planetary boundary layers. *Quart. J. Roy. Met. Soc.* **129**, 3339-3356.

Table 1. LES estimates of empirical constants

Constant	Empirical value	In formula	Equation number
C_0	0.67	$u_T = u_*^2(1 + C_0 \mu_\Gamma)$	(11)
C_{NM}	0.1	$\frac{1}{L_{\{M,H\}}} = \left[\left(\frac{1}{L} \right)^2 + \left(\frac{C_{\{NM,NH\}}}{L_N} \right)^2 + \left(\frac{C_{\{fM,fH\}}}{L_f} \right)^2 \right]^{1/2}$	(14)
C_{NH}	1.5		
C_{fM}	1		
C_{fH}	1		
C_u	2.5	$\frac{\partial u}{\partial z} = \frac{\tau^{1/2}}{kz} \left(1 + \frac{C_u z}{L_M} \right)$	(15)
k	0.47		
C_{NA}	0.09	$m_A = \left[\left(\frac{h}{L_s} \right)^2 + \left(\frac{C_{NA} h}{L_N} \right)^2 \right]^{1/2}$	(41)
C_{NB}	0.15	$m_B = \left[\left(\frac{h}{L_s} \right)^2 + \left(\frac{C_{NB} h}{L_N} \right)^2 \right]^{1/2}$	(42)
a	1.4	$A = -am_A + \ln(e^{A_0} + m_A)$	(44a)
A_0	0.5±0.9		
b	10	$B = B_0 + bm_B^2$	(44b)
B_0	1.5±0.5		
C_θ	2	$\frac{\partial \theta}{\partial z} = \frac{\theta_*}{k_T z} \left(1 + \frac{C_\theta z}{L_H} \right)$	(48)
k_T	0.47		
C_{NC}	1.2	$m_C = \left[\left(\frac{h}{L_s} \right)^2 + \left(\frac{C_{NC} h}{L_N} \right)^2 \right]^{1/2}$	(57)
c	4.1	$C = -cm_C + \ln(e^{C_0} + m_C) \approx -cm_C + C_0$	(56)
C_0	12		

Appendix: Self-similarity of the vertical profile of the momentum flux

In the nocturnal PBLs, the assumption of self-similarity of the vertical turbulent flux of momentum is consistent with the following scaling analysis of the Ekman equations. Taking $\tau/u_*^2 = f_\tau(\zeta)$ and $F_\theta/F_{\theta s} = f_{F\theta}(\zeta)$, the approximate eddy viscosity formulation Eq. (16) becomes $K_M = K_M^* f_{KM}(\zeta)$, where $K_M^* = kC_u^{-1}u_*L_s$ is a depth-constant eddy-viscosity scale and $f_{KM}(\zeta) = f_\tau^2 f_{F\theta}^{-1}$ is a universal function decreasing towards the PBL upper boundary [our LES-based analytical approximations give $f_{KM} = \exp(-10/3\zeta^2)$]. Then, differentiating Eq. (25) over z , multiplying by K_M , using the PBL height scale $h \sim (K_M^*/|f|)^{1/2}$ and going to dimensionless variables $\zeta = z/h$ and $\hat{\tau}_{\{x,y\}} = \tau_{\{x,y\}}/u_*^2$, yields

$$\hat{\tau}_y + f_{KM}(\zeta) \frac{\partial \hat{\tau}_x}{\partial \zeta} = 0, \quad -\hat{\tau}_x + f_{KM}(\zeta) \frac{\partial \hat{\tau}_y}{\partial \zeta} = 0.$$

The boundary conditions, Eq. (26), take the form $\hat{\tau}_x=1$, $\hat{\tau}_y=0$ at $\zeta=0$ and $\hat{\tau}_x=0$, $\hat{\tau}_y=0$ at $\zeta \rightarrow \infty$. Thus the problem becomes self-similar, which ensures that $\hat{\tau}_x$ and $\hat{\tau}_y$ are single-valued functions of ζ . Figure 1 confirms this conclusion and gives grounds to extend it to long-lived and conventionally neutral PBLs.

Figure captions

Figure 1. Normalised vertical profiles: (a) turbulent flux of momentum τ/u_*^2 , (b) turbulent flux of potential temperature F_θ/F_{θ_s} , (c) length scale L/L_s , and (d) temperature scale θ_*/θ_{*s} . The dimensionless height $\zeta = z/h$ is based on the PBL depth h . LES data represent nocturnal (crosses), long-lived (circles) and conventionally neutral (squares) PBLs. The lines are (a) $\tau/u_*^2 = \exp(-\frac{8}{3}\zeta^2)$ or $(1-\zeta)^{3/2}$; (b) $F_\theta/F_{\theta_s} = \exp(-2\zeta^2)$ or $(1-\zeta)$; (c) $L/L_s = \exp(-2\zeta^2)$ or $(1-\zeta)^{5/4}$; (d) $\theta_*/\theta_{*s} = \exp(-\frac{2}{3}\zeta^2)$ or $(1-\zeta)^{1/4}$. Solid and dashed lines represent exponential- and power-law approximations, respectively.

Figure 2. Dimensionless velocity gradient $\Phi_M = \frac{kz}{\tau^{1/2}} \frac{\partial u}{\partial z}$ versus alternative dimensionless heights based on different z -dependent turbulent length scales: (a) z/L , Eq. (12a); (b) z/L_M , Eq. (14) with $C_{NM} = 0.1$, $C_{fM} = 1$. LES data represent three different types of the stable PBLs: nocturnal (crosses), long-lived (circles) and conventionally neutral (squares). The lines are (a) traditional scaling $\Phi_M = 1 + 2.5z/L$; (b) multi-limit scaling $\Phi_M = 1 + 2.5z/L_M$. The best fit is achieved with $k=0.47$.

Figure 3. LES data on the geostrophic-drag resistance-law coefficient $A = \ln \frac{h}{z_{0u}} - k \frac{u_g}{u_*}$ (with $k=0.47$) versus the composite stratification parameter m_A , Eq. (41), with $C_{NA} = 0.09$. Data points \times , \circ and \square represent new LES for nocturnal, long-lived and conventionally neutral PBLs, respectively. Earlier LES data, namely, \diamond (Brown *et al.*, 1994) and \star (Kosovic and Curry, 2000) does not show any systematic deviations from new LES. Larger spread in old data from Brown *et al.* (1994) is only natural because of inevitably lower quality of the LES of that time. Error bars in Figure 3a show the ± 3 standard deviation intervals for each LES run (with 96% statistical confidence). Figure 3b employing semi-log coordinates demonstrates how the theory performs in near-neutral and moderate-stability regimes. The line is $A = -1.4m_A + \ln(e^{0.5} + m_A)$.

Figure 4. Same as in Figure 3, but for the cross-isobaric-angle resistance-law coefficient $B = k \frac{v_g}{fh}$ (with $k=0.47$) versus m_B , Eq. (42), with $C_{NB} = 0.15$. The line is $B = 1.5 + 10m_B^2$. Notice that data points \diamond are taken from old and lower quality LES, which causes their large spread.

Figure 5. The dimensionless potential temperature gradient $\Phi_H = \frac{k_T \tau^{1/2} z}{-F_\theta} \frac{\partial \theta}{\partial z}$ versus alternative dimensionless heights: (a) z/L and (b) z/L_H with $C_{NH} = 1.5$ and $C_{fH} = 1$. Crosses and circles represent nocturnal and long-lived PBLs, respectively. Data on conventionally neutral PBLs are not included. The lines are: (a) $\Phi_H = 1 + 2z/L$; (b) $\Phi_H = 1 + 2z/L_H$. The best fit is achieved with $k_T = 0.47$.

Figure 6. Same as in Figures 3 and 4, but for the potential-temperature resistance-law coefficient $C = \ln \frac{h}{z_{0u}} - k_T \frac{\Delta \theta_{PBL}}{\theta_{*s}}$ (with $k_T = 0.47$) versus m_C , Eq. (57) with $C_{NC} = 1.2$. Data points \times and \circ represent new LES for nocturnal and long-lived PBLs, respectively. LES data for conventionally neutral PBLs are not included (here $\theta_{*s} \rightarrow 0$, which is why the temperature resistance law loses physical meaning). The line is $C = -4.1m_C + \ln(e^{12} + m_C)$.

Figure 7. The ratio $Q_E = \int_0^h E^{SGS} dz / \int_0^h E^{RES} dz$ of the sub-grid to the resolved portions of the turbulent kinetic energy as dependent on the dimensionless vertical resolution Δ_z/L_M . The smaller are Q_E and Δ_z/L_M , the higher is the quality of the LES run.

Figure 8. Temporal evolution of the resistance-law coefficients A_0 , B_0 and the PBL depth h_{PBL} in the LES-generated truly neutral PBL ($G = 5 \text{ m s}^{-1}$, $z_{0u} = 0.1 \text{ m}$, $f = 10^{-4} \text{ s}^{-1}$, $F_{\theta s} = 0$, $N = 0$). Squares show mean values averaged over one-hour intervals. Error bars show the ± 3 standard deviation intervals for each hour. The sold line shows filtered 10-minute data.

Figure 9. Same as in Figure 8, but for the resistance-law coefficients A , B , C and the PBL depth h_{PBL} in the LES-generated long-lived stable PBL ($G = 5 \text{ m s}^{-1}$, $z_{0u} = 0.1 \text{ m}$, $f = 10^{-4} \text{ s}^{-1}$, $F_{\theta s} = 0.005 \text{ K m s}^{-1}$, $N = 0.01 \text{ s}^{-1}$).

Figure 10. Traditional presentation of the geostrophic-drag resistance-law coefficient $\tilde{A} \equiv A - \ln(|f|h_E/u_*)$ as a single-valued function of the internal stability parameter $\mu = u_*|f|L$. Data points are taken from different sources: \times , \circ and \square are new LES data for the nocturnal, long-lived and conventionally neutral PBLs, respectively; \diamond and \star are earlier LES data from Brown *et al.* (1994) and Kosovic and Curry (2000), respectively; other symbols are field data: * Cabauw (Nieuwstadt, 1981), Δ Wangara (Yamada, 1976), + different Russian sites (Zilitinkevich and Chalikov, 1968). The curves show old analytical approximations (summarised by Byun, 1991): — Vachot and Musson-Genon, — — Arya, — • — Long and Guffey, —+— Brost and Wyngaard, —◇— Derbyshire. Error bars show the ± 3 standard deviation intervals.

Figure 11. Same as in Figure 10, but for the cross-isobaric-angle resistance-law coefficient $\tilde{B}(\mu) \equiv (|f|h_E/u_*)B$.

Figure 12. Same as in Figures 10 and 11, but for the temperature resistance-law coefficient $\tilde{C}(\mu) \equiv C - \ln(|f|h_E/u_*)$.

Figure 13. LES data on the geostrophic-drag resistance-law coefficient in truly neutral stratification $A_0 = A|_{m \rightarrow 0}$ versus the surface Rossby number $G/|f|z_{0u}$. The line is $A_0 = 0.51$.

Figure 14. Same as in Fig. 13, but for the cross-isobaric-angle coefficient $B_0 = B|_{m \rightarrow 0}$. The line is $B_0 = 1.5$.

Figure 1

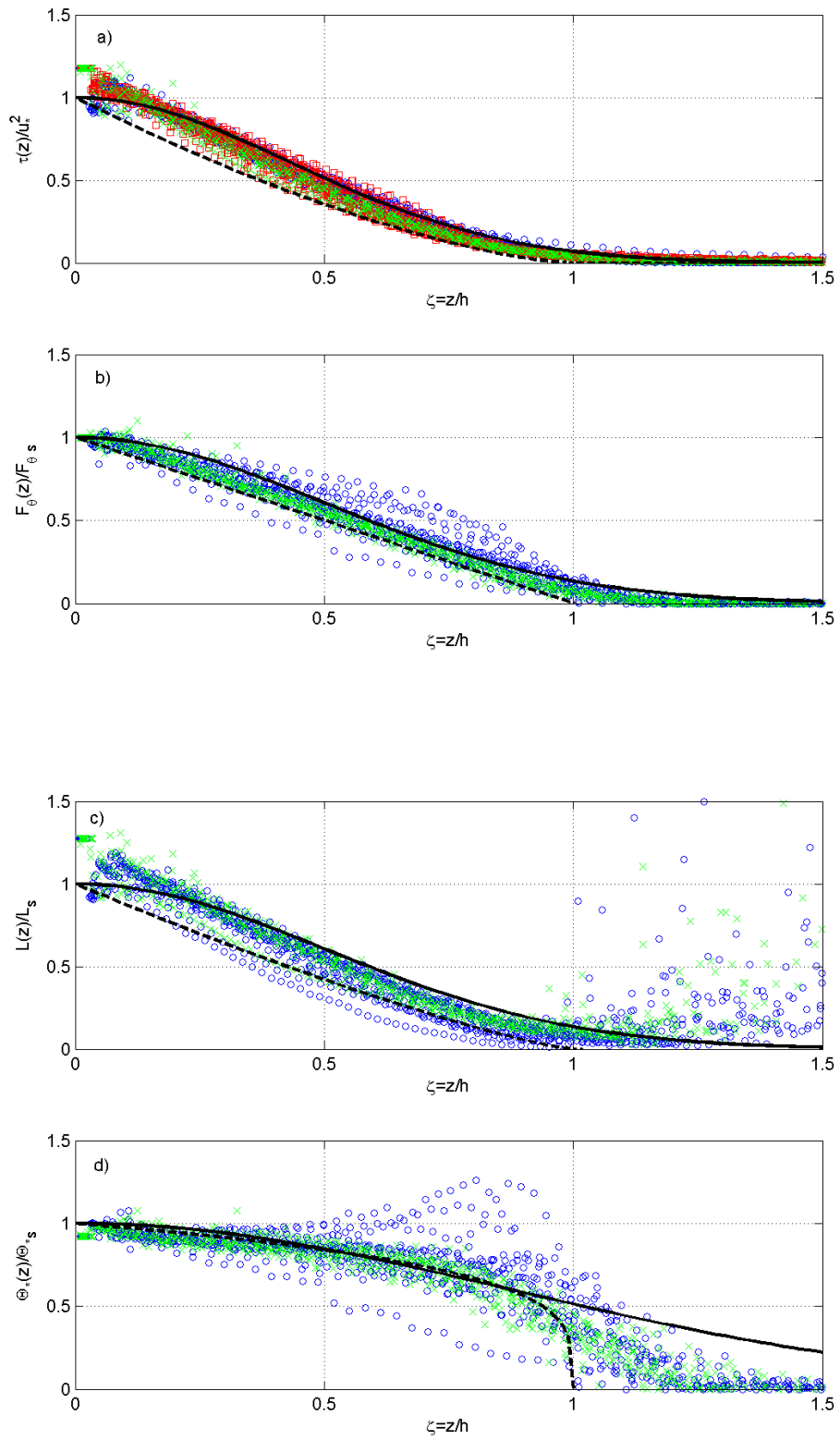


Figure 2

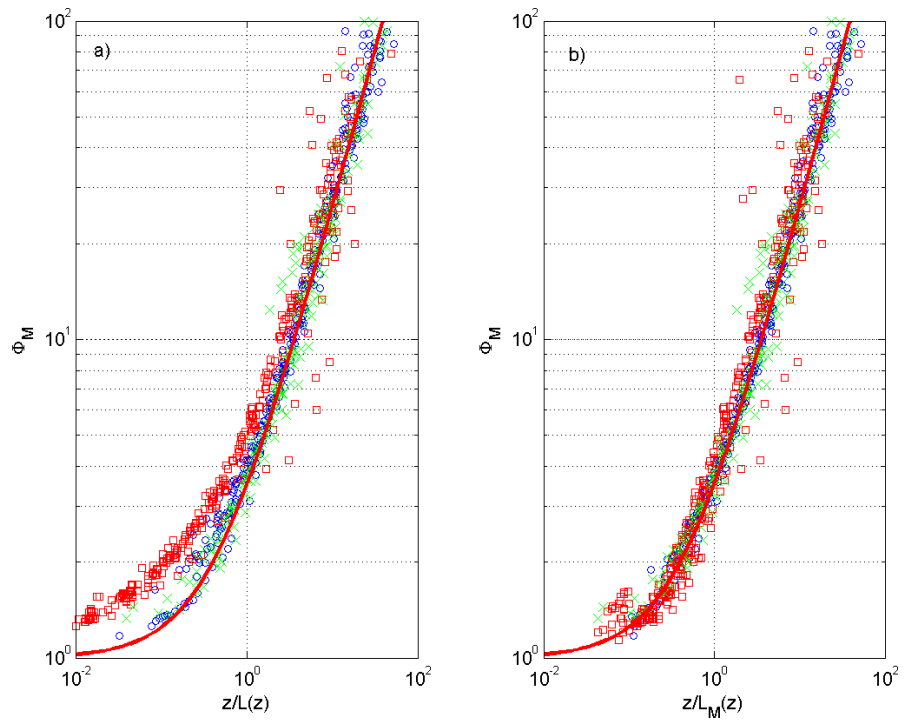


Figure 3

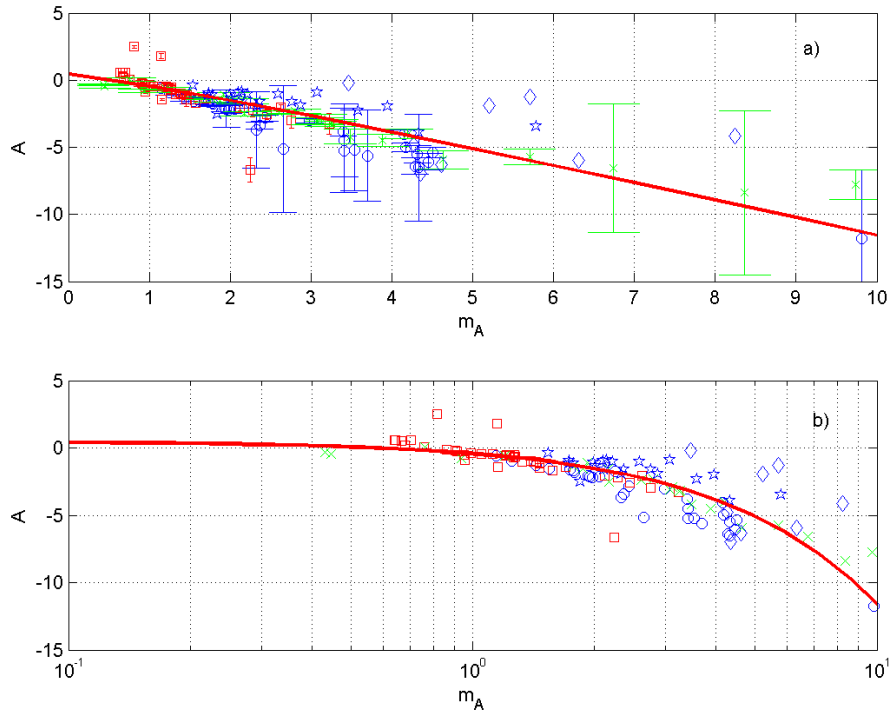


Figure 4

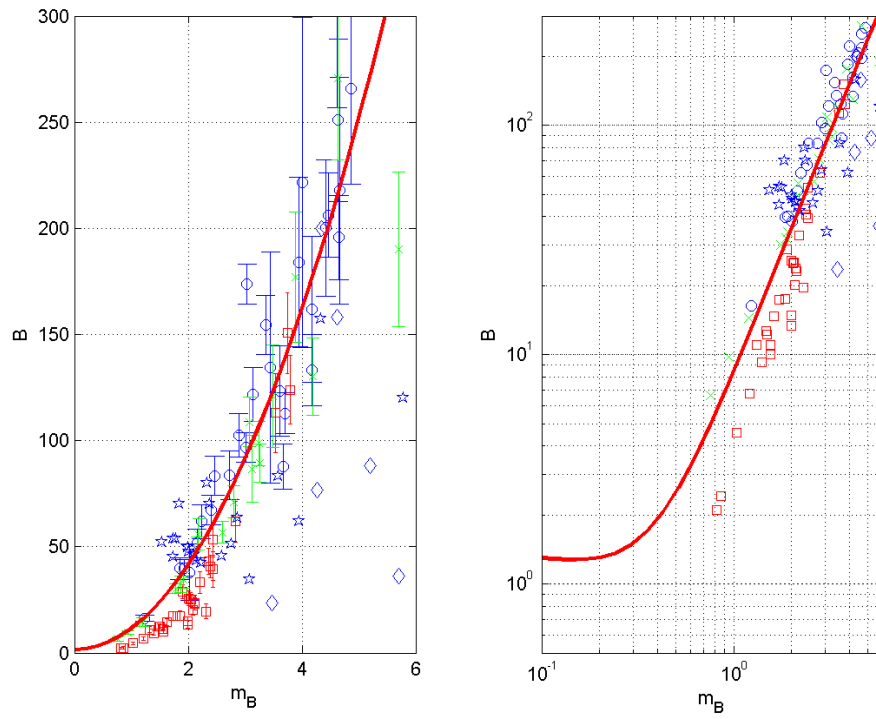


Figure 5

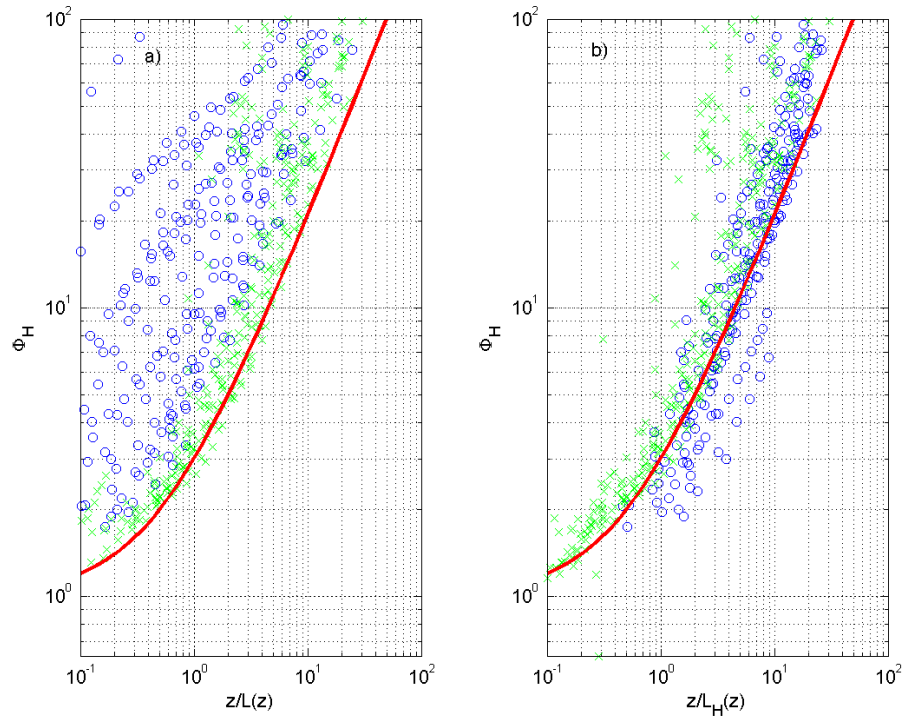


Figure 6

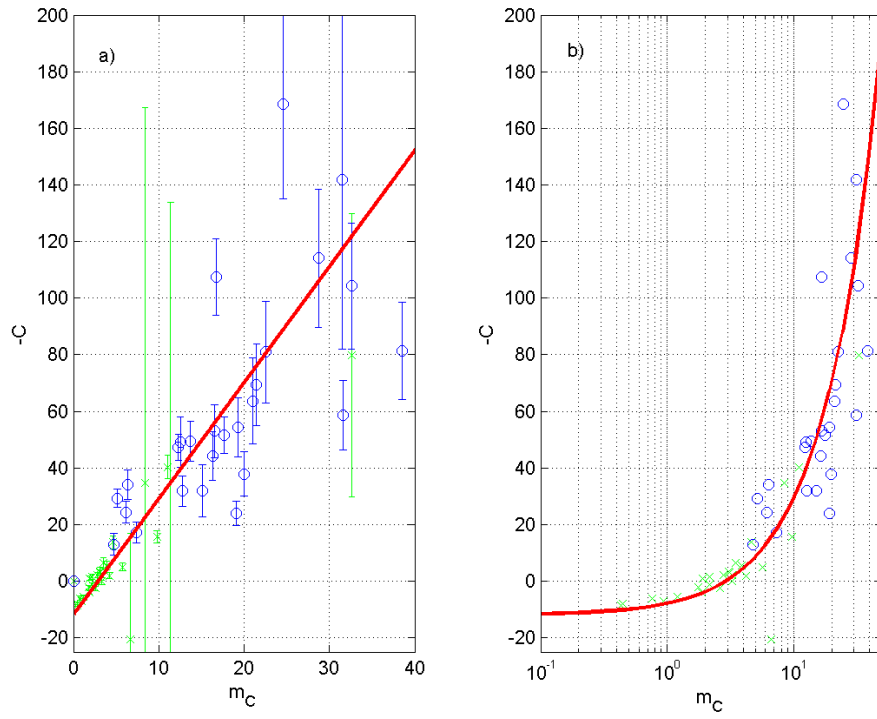


Figure 8

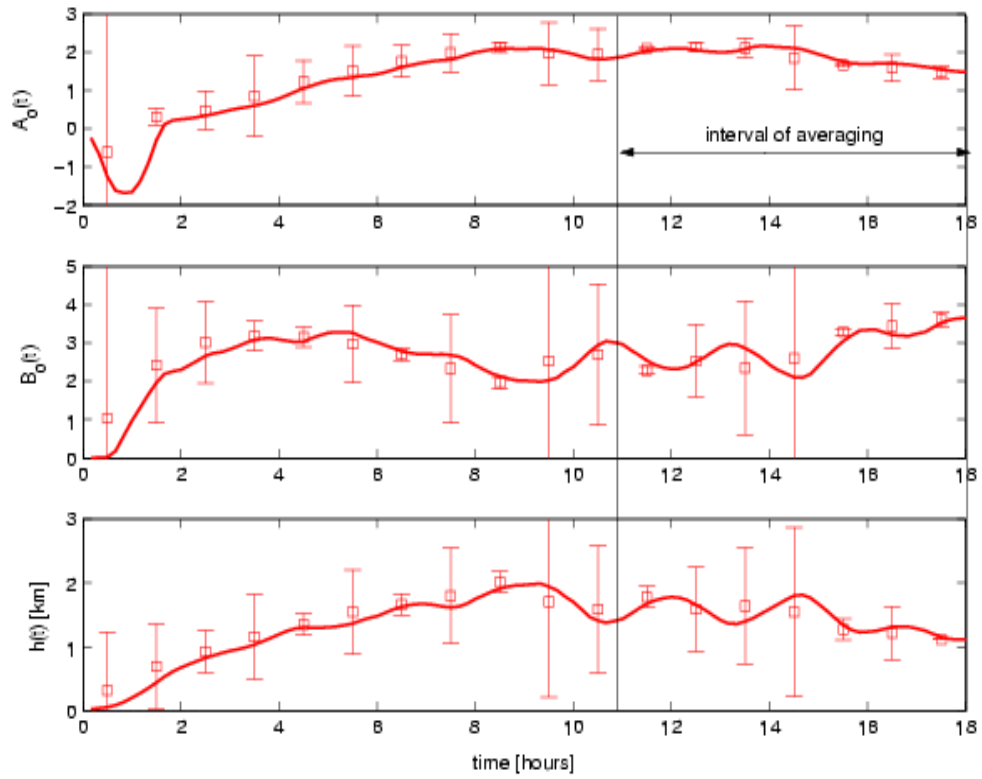


Figure 9

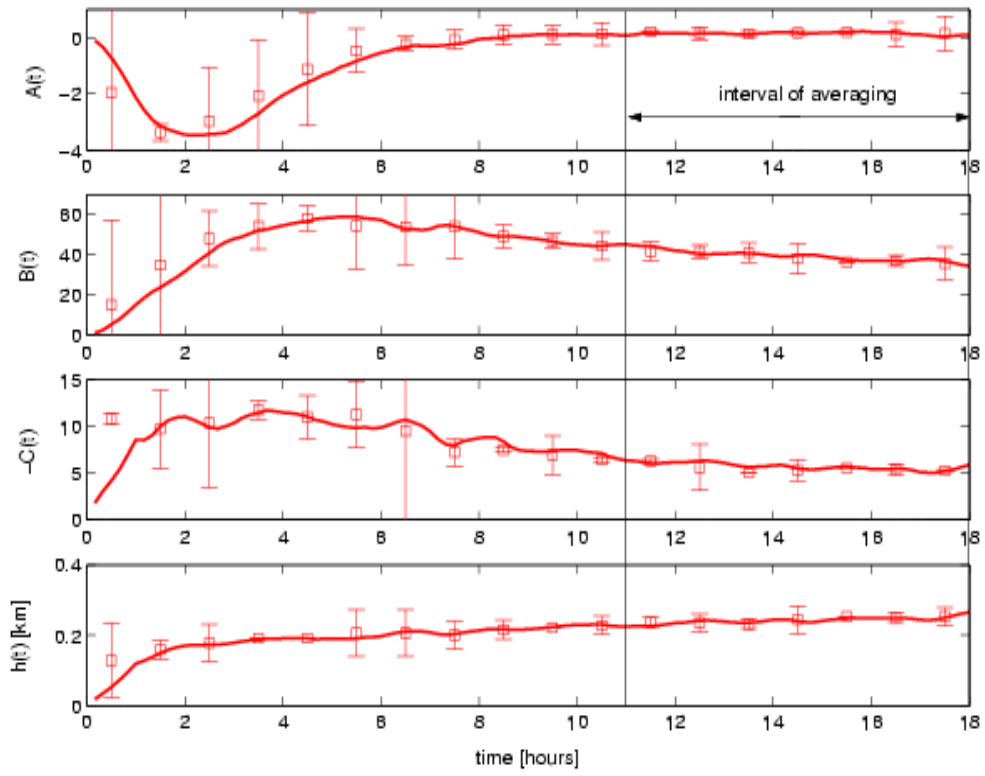


Figure 10

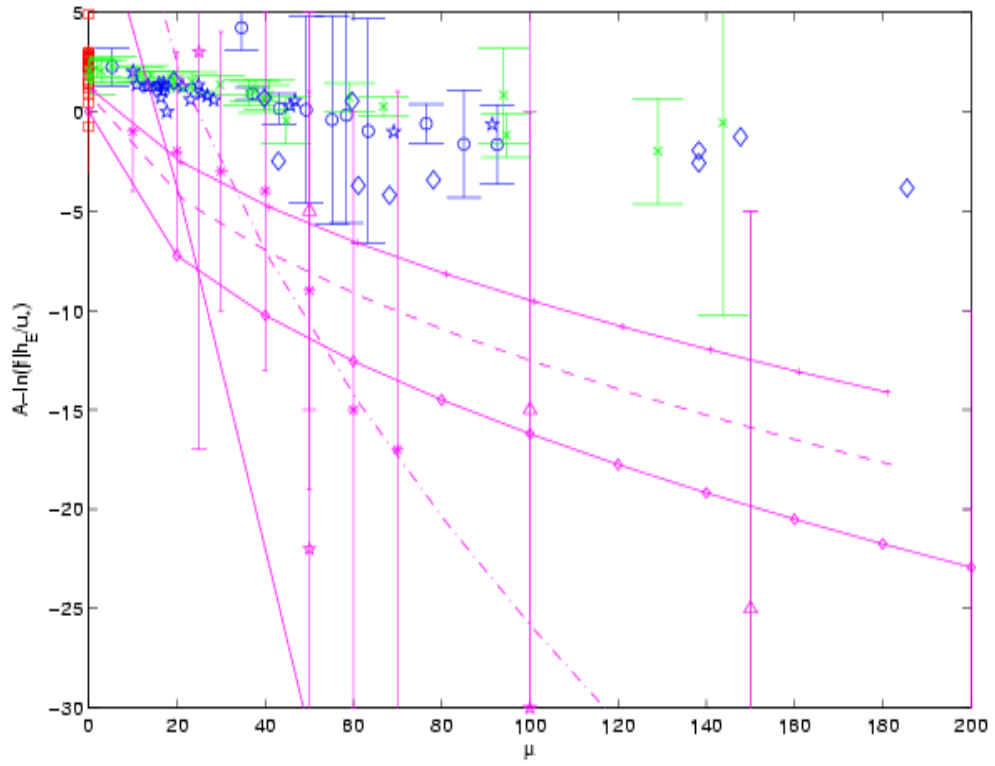


Figure 11

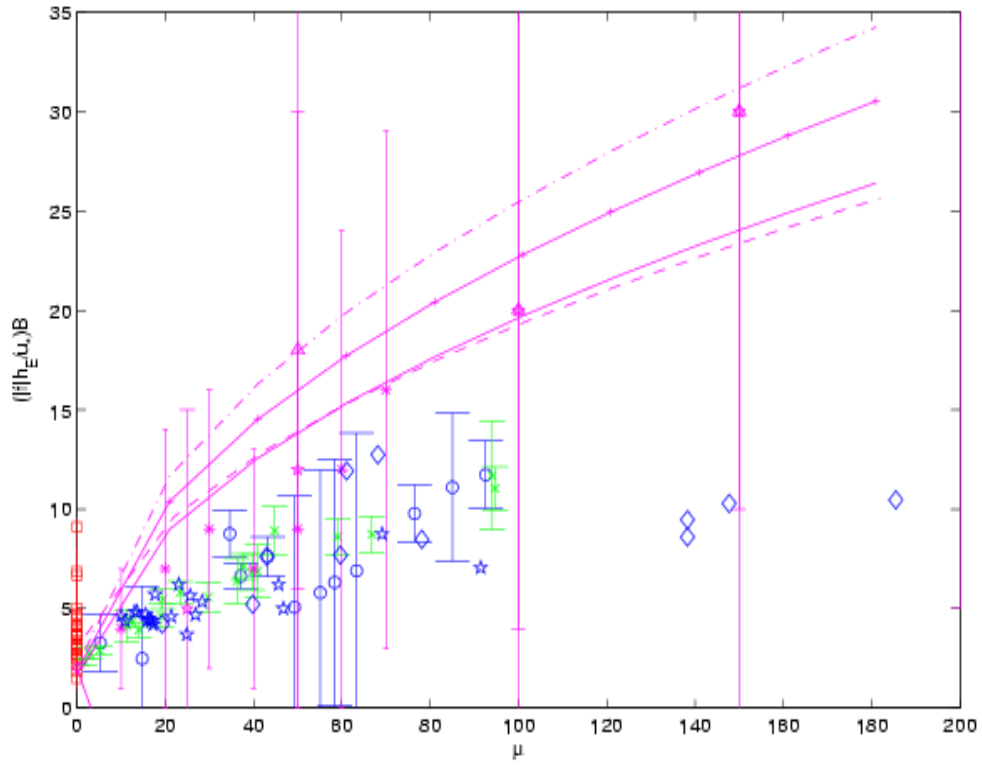


Figure 12

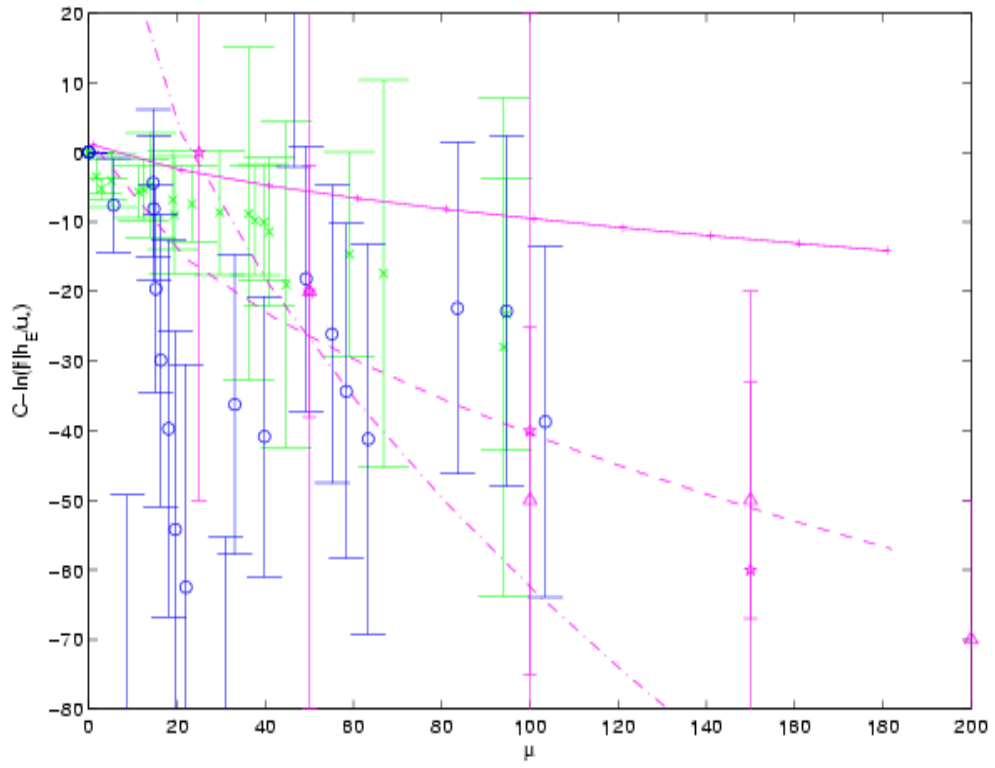


Figure 13

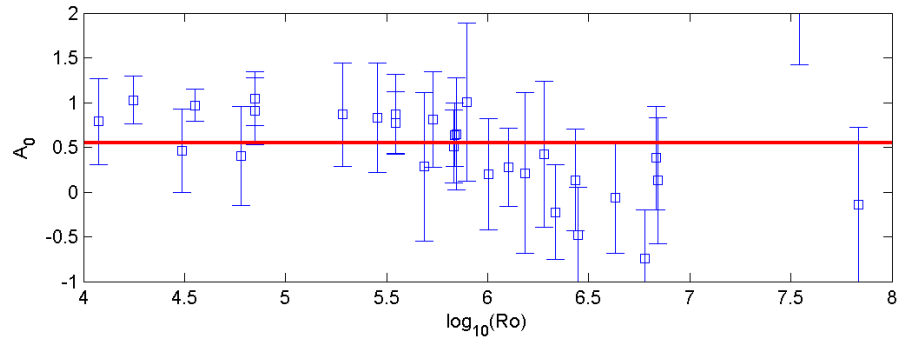


Figure 14

